Journal of The Electrochemical Society, 2021 **168** 042502
1945-7111/2021/168(4)/042502/20/$40.00 © 2021 The Electrochemical Society ("ECS"). Published on behalf of ECS by IOP Publishing Limited

Review—The Emerging Technologies for Producing Low-Cost Titanium

Ramana G. Reddy,[z] Pravin S. Shinde, and Aimin Liu

Department of Metallurgical and Materials Engineering, The University of Alabama, Tuscaloosa 35487, United States of America

This paper presents a thorough review of various technologies to obtain titanium and its alloys and their discussion concerning their merits and demerits. Titanium and its alloys are ideal advanced structural materials because of their excellent properties such as high corrosion resistance, exceptional strength-to-weight ratio, bio-compatible, non-magnetic and mechanical properties. As a result, such materials are served extensively for several engineering applications that include wind turbines, auto industries, biomedical implants, aerospace industry, marine structures, and many others. However, the low yield and higher cost production of the current employed energy-intensive Kroll process restricts the widespread use of titanium and its alloys. Numerous alternative extraction processes have been developed during the last few decades to produce titanium and its alloys in a more accessible and cost-effective way. Amid growing demand for titanium in the market, it is necessary to consider the impact of technological innovations that can reduce titanium production cost. Recent research and developments on the electrochemical reduction method of titanium production from molten salts or ionic liquids have shown promising results. This paper reviews the developments on titanium production and its alloys by various techniques, including but not limited to molten salt electrolysis processes, such as the FFC-Cambridge process, the OS process, the USTB process, and ionic-liquid electrolysis.
 [DOI: 10.1149/1945-7111/abe50d]

Manuscript submitted December 10, 2020; revised manuscript received February 5, 2021. Published April 1, 2021.

Titanium (Ti) metal is the ninth most abundant element present in the Earth's crust at a level of about 0.6%. Ti is commonly found in the form of rutile (TiO_2) and ilmenite ($FeTiO_3$) and is the fourth most abundant structural metal after aluminum (Al), iron (Fe), and magnesium (Mg).[1] Ti metal is exceedingly valued for its high strength-to-weight ratio and corrosion resistance and is advantageous at a wide range of temperatures. Titanium is equally strong as steel but with much less density. Therefore, it is essential as an alloying agent with many metals, including aluminum, molybdenum, and iron. These alloys find widespread applications in the aerospace industry (aircraft, spacecraft, engines, and missiles), accounting for 60%–75% usage because of their low density and their high tolerance for different working condition (extreme temperatures, creep, strength-weight ratio, etc.).[2,3] Being light-weight, Ti can provide more significant lifetime energy savings in transportation applications. Ti-alloys with other elements like aluminum and vanadium (Ti_6Al_4V) are particularly very crucial for medical devices in the biomedical industry as body implants.[4,5] Ti and its alloys are also used to manufacture high-end sports equipment such as bicycle frames and golf clubs because of its low density compared to steel and its stiffness compared to aluminum. However, all such pieces of equipment and devices are expensive due to the metal extraction cost using meticulous process techniques that involve high materials loss and high-energy consumption processing conditions.[6]

Reverend William Gregor discovered metal titanium in the year 1790. Still, the extraction of pure titanium on commercial scales (91 Kg) began in 1948 by DuPont and the US Bureau of Mines using the Kroll process. As seen in Table I, the world production of titanium sponge was 210 thousand metric tons in 2019, much lower than that of aluminum, magnesium, and iron. On the other hand, the metal titanium price, range from $9.10–9.50 per kg in 2015–2019, is relatively high compared to other metals. Therefore, the titanium metal consumption has been limited to aerospace applications (estimated 80% in 2019) because of low production and high price.[7]

The history of commercial production of Ti only dates back to 70 years, which makes it a new metal compared with commonly utilized metals like Fe, Al, and Cu. Because of Ti's strong affinity toward elements like C, N, S, and O, its extraction becomes very difficult and requires higher energy conditions, raising the production cost.[8,9] Despite its abundance, Ti is expensive because it is difficult to isolate from its ores. Titanium products have not been commercialized yet due to energy-intensive and costly titanium production requirements. Therefore, production cost reduction has been the objective of many research industries over the past few decades. If titanium's production cost falls dramatically, titanium could potentially replace the widely utilized stainless steel (leads the global production in 2019, Table I), leading to opening a significant market demand. Hence, titanium is considered as a material of the future, whose production could significantly be scaled up by technological innovations with cost reductions, thereby making it a general-purpose metal.[10,11] Over the past three decades, various novel technologies have emerged to produce titanium with lower cost and lower energy consumption than the Kroll process. Electrolysis in molten salts with the starting materials of TiO_2 or $TiCl_4$ has been considered a promising method, including the FFC process,[12] the OS process,[13] the electrolysis of titanium oxycarbides (the USTB process),[14] and the electrolysis from room-temperature ionic liquids.[15]

In this paper, the Hunter and Kroll processes are described briefly, and then a review on the developments of producing titanium and its alloys from various molten salts is presented. Furthermore, the different reaction mechanisms for various processes are discussed. Since the temperature is one of the factors causing the high Ti production cost, the research topics are mainly divided into two aspects based on the different operating temperatures. One involves using high-temperature molten salts (e.g., NaF-KF, Na_3AlF_6, NaCl-KCl, and $CaCl_2$, etc.), while the other utilizes room-temperature molten salts (e.g., $AlCl_3$-EmimCl, $AlCl_3$-BmimCl, and $AlCl_3$-BPC, etc.) at low temperatures. All the low- and high-temperature Ti production processes are summarized with their main features, advantages, and disadvantages. A more emphasis is given to obtaining titanium from low-cost and efficient methods of fabrication. Some of the recent reviews and book chapters[10,16,17] referred to in this paper could help understand the working principles of the Kroll process, HAMR process, USTB process, and other alternative processes. This review article would be of interest to a broad readership of chemists, physicists, materials scientists, and chemical engineers for future advancements in the field.

Hunter Process and Kroll Process

The Hunter process, invented in 1910 by Matthew A. Hunter, was the first industrial method of producing titanium.[18] According to reaction (1), purified titanium chloride ($TiCl_4$) is produced by chlorinating rutile (TiO_2) in a fluidized bed reactor at about 1000 °C to

[z]E-mail: rreddy@eng.ua.edu

Table I. World production (excludes US production) of Fe, Al, Mg, and Ti in 2019 and market price in recent five years (2015–2019).

Metal	World production (thousand metric tons)	Market price per kilogram (dollars)
Iron and steel (Fe)	1,300,000	0.20–0.35
Aluminum (Al)	64,000	1.77–2.54
Magnesium (Mg)	1100	1.83–2.53 (No data for 2019)
Titanium (Ti)	210	9.10–9.50

provide raw $TiCl_4$ that is further refined through fractional distillation to remove metal chlorides impurities such as $AlCl_3$, $SiCl_4$, $FeCl_3$, and $VOCl_3$. In the Hunter process, titanium is produced via the reaction between the sodium (Na) and a small excess of $TiCl_4$ according to reaction (2) at 900 °C in a sealed retort.

magnesium (Mg). According to reaction (3), the products were titanium metal along with $MgCl_2$ salts and unreacted Mg. After 2–5 days of reduction reaction, the vacuum is applied to the retort to remove the $MgCl_2$ salts and excess Mg.[21] In addition, Mg and Cl_2 are regenerated from the recycled $MgCl_2$ salts in a separate electrolysis cell.

$$\text{Chlorination: } TiO_2 + 2\,Cl_2 + (1 + x)C = TiCl_4 + (1 + x)CO_{(2-x)} (\text{where } x = 0 \text{ or } 1) \quad [1]$$

$$\text{Reduction: } TiCl_4 + 4\ Na = Ti + 4\ NaCl \quad [2]$$

The final product would be a NaCl-titanium mixture. However, sodium and $TiCl_4$ are soluble in NaCl. Thus, it is not practical to drain off the NaCl during the reduction process. When the reduction is finished, the products would have to be chipped out, crushed, leached (with hydrochloric acid), and washed.[19] The retort is also considerably large because it contains 10.8 cm^3 of NaCl for every 1 cm^3 of titanium. The Hunter process was later replaced by a more economical method that used recyclable magnesium (Mg) in place of sodium, which is known as the Kroll process.

The Kroll process, which is currently the primary commercial process for titanium production, was developed by William J. Kroll in Luxembourg in 1937. As shown in Fig. 1,[20] the Kroll process first converts TiO_2 to $TiCl_4$ (g) by reacting the titanium ores with carbon (C) and chlorine gas (Cl_2) in a fluidized bed at 1000 °C, according to the reaction (1). After subsequent purification through fractional distillation at 127 °C, $TiCl_4$ was fed into an argon-filled retort at 800 °C–900 °C, where it is reduced to metal titanium by 15%–30% excess liquid

$$\text{The Kroll process: } TiCl_4 + 2Mg = Ti + 2MgCl_2 \quad [3]$$

Although the Kroll process has been applied to industrial production for many decades, there are many disadvantages that include toxic Cl_2 gas, expensive reductant Mg, long process route, low productivity, and high energy consumption (71.61 kWh kg^{-1} Ti).[17]

High-Temperature Molten Salt Electrolysis

NaF-KF, LiF-NaF-KF molten salts electrolysis.—It was reported by Stetson (1963)[22] that the Ti electrodeposits could be obtained at 850 °C from NaF-KF melts containing K_2TiF_6. However, a layer of insoluble lower-valent titanium salts composed of Ti^{3+} was found to contact the cathode. Clayton et al. (1973)[23] investigated the electrochemistry of K_2TiF_6 in LiF-NaF-KF eutectic molten salts at 500 °C. It was found that Ti^{4+} species is reversibly reduced to Ti^{3+} at −0.058 V vs a Ni^{2+} (saturated)/Ni reference electrode, while the reduction of Ti^{3+} to metal titanium proceed reversibly at −1.798 V.

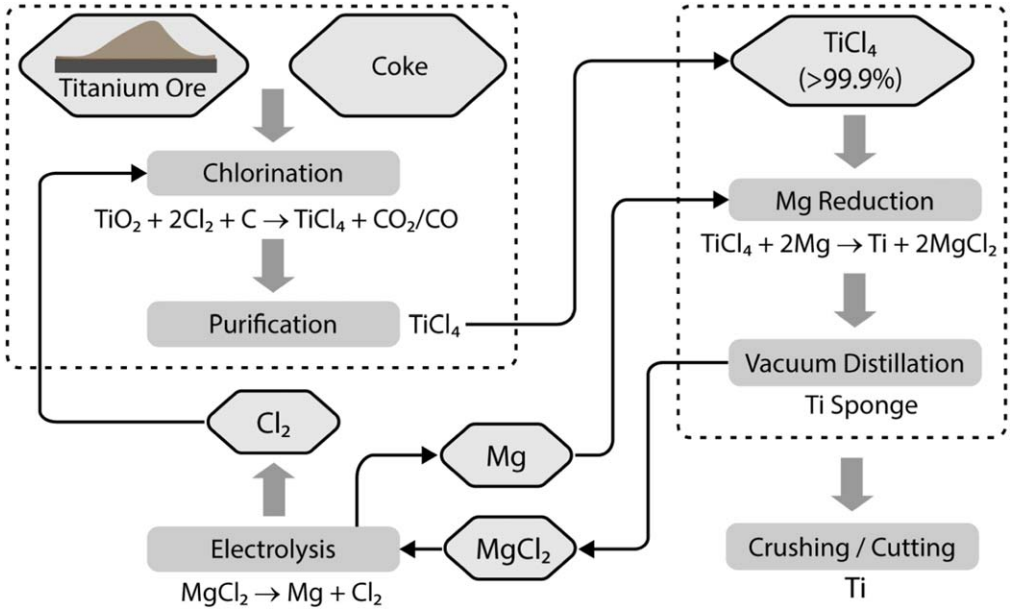

Figure 1. Schematic flowchart of the Kroll process.[20]

Table II. Solubility of TiO_2 in molten cryolite and Na_3AlF_6 and Na_3AlF_6-Al_2O_3 at 1020 °C reported in the literature.

Molten salts	wt.% TiO_2	References
Na_3AlF_6	6.1	Hayakawa and Kido (1952)[37]
Na_3AlF_6	5.7	Belyaev et al. (1956)[38]
Na_3AlF_6−5wt%Al_2O_3	5.0	Belyaev et al. (1956)[38]
Na_3AlF_6	5.2	Madhavan et al. (1971)[39]
Na_3AlF_6	6.5	Sterten and Skar (1988)[40]
Na_3AlF_6	5.3	Qiu et al. (1988)[34]
Na_3AlF_6	5.2	Jentofsten et al. (2002)[41]

Similar observations were reported by Lepinay et al. (1986)[24] in LiF-KF and LiF-NaF-KF eutectic melts containing K_2TiF_6 at temperatures between 550 and 850 °C. According to results from cyclic voltammetry, Ti^{4+} species (TiF_6^{2-}) were first reduced to Ti^{3+} species (TiF_6^{3-}), then Ti^{3+} species were reduced to metal titanium. That indicates, the reduction mechanism proceeds via two reversible steps according to reactions (4) and (5). In addition, adherent coatings of pure titanium with a thickness of 30 μm per hour were obtained in the form of copper-titanium solid solutions such as Cu_4Ti, Cu_3Ti_2, TiCu, and Ti_2Cu.

$$TiF_6^{2-} + e^- \rightarrow TiF_6^{3-} \quad [4]$$

$$TiF_6^{3-} + 3e^- \rightarrow Ti + 6F^- \quad [5]$$

As an extension to Lepinay's work, Robin et al.[25–30] conducted numerous studies on the mechanisms of titanium electrodeposition on iron and nickel electrodes in LiF-NaF-KF eutectic melts. They studied the interactions between titanium and the substrate. It was reported that Ti^{3+} species (TiF_6^{3-}) were reduced to pure metal titanium via a single three-electron exchange step at iron electrodes in the temperature range of 600 °C–700 °C. According to reactions (6)–(8), a 20–30 μm thick coating of pure titanium was obtained in the form of nickel-based alloys such as Ni_3Ti, TiNi, Ti_2Ni, and pure titanium external coating.[27] Besides, the diffusion coefficients for TiF_6^{3-} at temperature of 600 °C–900 °C are determined by 1.4×10^{-2} exp (−6154/T).[25,28] The authors[29,30] also reported pure dendritic titanium deposits from K_3TiF_6-LiF-NaF-KF at 750 °C with high current efficiencies (80%–85%). In comparison, FeTi and Fe_2Ti intermetallic compounds were obtained at 800 °C and 900 °C with low current efficiencies (<55%) according to reactions (9)–(10).

$$TiF_6^{3-} + 3Ni + 3e^- \rightarrow TiNi_3 + 6F^- \quad [6]$$

$$2TiF_6^{3-} + TiNi_3 + 6e^- \rightarrow 3TiNi + 12F^- \quad [7]$$

$$TiF_6^{3-} + TiNi + 3e^- \rightarrow Ti_2Ni + 6F^- \quad [8]$$

$$TiF_6^{3-} + 2Fe + 3e^- \rightarrow Fe_2Ti + 6F^- \quad [9]$$

$$TiF_6^{3-} + Fe_2Ni + 3e^- \rightarrow 2FeTi + 6F^- \quad [10]$$

To produce TiB_2 coatings, an attractive material for the aluminum industry as cathode lining materials, Li et al. (2006)[31,32] investigated the mechanism of the electrochemical reduction of K_2TiF_6 on Pt electrode in LiF-NaF-KF eutectic molten salts at 700 °C. The electrochemical reduction of Ti^{4+} was found to proceed by a reversible three-step process [$Ti^{4+} \rightarrow Ti^{3+} \rightarrow Ti^{+} \rightarrow Ti^{0}$], and the electro-crystallization process is instantaneous.

Cryolite-based (Na_3AlF_6) molten salts electrolysis.—Although titanium is considered a detrimental impurity in the Hall-Héroult bath that reduces the current efficiency and the purity of aluminum products,[33] it is feasible to produce Al-Ti alloy in the aluminum electrolysis cells.

Qiu et al. (1988)[34] prepared Al-Ti alloys with a titanium content of less than 2wt.% from synthetic rutile (92 wt.% TiO_2) by electrolysis in Na_3AlF_6-Al_2O_3 melts. Liu et al. (2002)[35] conducted an electrolysis experiment by adding a mixture of TiO_2 (purity 98wt.%) and Al_2O_3 powders into the industry electrolyzers and Al-Ti alloy with a titanium content of less than 0.30wt.% can be produced without significant loss of current efficiency.

Yu et al. (2004)[36] produced Al-Ti alloy on liquid aluminum cathode by molten salt electrolysis in 93wt.% Na_3AlF_6−5wt.% Al_2O_3−2wt.%TiO_2 melts at 960 °C for 68 min, and it was found that titanium content in the Al-Ti alloy was over 9wt.%. As shown in Eqs. 11 and 12, there are two primary reaction mechanisms involved in the extraction of titanium: (i) the Hall-Heroult process for deposition of aluminum and titanium by electrolysis; (ii) the reduction of TiO_2 by aluminum.

$$(\text{Electrodeposition process})\ Al^{3+} + Ti^{4+} + 7e = Al + Ti \quad [11]$$

$$(\text{Thermal reduction by Aluminium})\ Al + Ti^{4+} = Al^{3+} + Ti \quad [12]$$

$$2AlF_6^{3-} + TiO_2 \rightarrow TiOF_x^{2-x} + Al_2OF_6^{2-} + (6-x)F^- \quad [13]$$

As seen in Table II, the solubility of TiO_2 in Na_3AlF_6 and Na_3AlF_6−5wt.%Al_2O_3 have been measured by several researchers.[34,37–41] According to Jentofsten et al. (2002),[41] the

Table III. Summary of the electrochemical mechanisms of titanium species in various cryolite-based molten salts and at different working electrodes.

Molten salts	Working electrode	Reduction mechanism	References
Na_3AlF_6-TiO_2	Graphite	$Ti^{4+} \rightarrow Ti^{0}$	Qiu et al. (1988)[34]
Na_3AlF_6-$CaTiO_3$	Platinum (Pt)	$Ti^{4+} \rightarrow Ti^{0}$	Devyatkin et al. (1998)[43]
Na_3AlF_6-Al_2O_3-TiO_2	Platinum (Pt)	$Ti^{4+} \rightarrow Ti^{3+} \rightarrow Ti^{0}$	Devyatkin et al. (1998)[43]
Na_3AlF_6-TiO_2	Graphite Aluminium (Al)	$Ti^{4+} \rightarrow Ti^{2+} \rightarrow Ti^{0}$ $Ti^{4+} \rightarrow Ti^{0}$	Qin et al. (2006)[44]
Na_3AlF_6-AlF_3-TiO_2	Tungsten (W)	$Ti^{4+} \rightarrow Ti^{2+} \rightarrow Ti^{0}$	Sun et al. (2008)[45]

solubility of TiO_2 in Na_3AlF_6 melts at 1020 °C was reported to be 5.2 wt%, which is in good agreement with the findings of Madhavan et al. (1971)[39] and Qiu et al. (1988).[34] In addition, Jentofsten et al. (2002)[41] pointed out that the most probable titanium species in cryolite melts are $TiOF_2$ and Na_2TiO_3. Sterten and Skar (1988)[40] also studied the dissolution mechanism of TiO_2 in cryolite using thermal and chemical analysis, and they suggested that the most probable dissolution process is:

Recently, Yan et al. (2016)[42] attempted producing pure titanium through molten salt electrolysis in Na_3AlF_6-TiO_2 at 1050 °C. It was concluded that pure titanium could not be made from only TiO_2 dissolved in cryolite, and TiO_2 was partially reduced to low valence states such as Ti_3O_5 and Ti_4O_7. However, Al-Ti compounds ($TiAl_3$, TiAl, and Ti_3Al) can be produced by electrolysis with aluminum's addition into cryolite-TiO_2 melts. Devyatkin et al. (1998)[43] suggested that $CaTiO_3$ was a potential raw material to produce Al-Ti alloys in Hall-Héroult cells, and the reduction of $CaTiO_3$ to titanium proceeded by one irreversible step [$Ti^{4+} \rightarrow Ti^0$].

In addition, the electrochemical behavior of TiO_2 in cryolite molten salt was investigated on different electrodes.[34,43–46] As a summary in Table III, Qiu et al. (1988)[34] studied the deposition of titanium on graphite electrode in Na_3AlF_6−0.5wt.%TiO_2 melts at 1050 °C by cyclic voltammetry, and the results showed that titanium is deposited in one-step [$Ti^{4+} \rightarrow Ti^0$]. According to Devyatkin et al. (1998),[43] the deposition of titanium on the Pt electrode in Na_3AlF_6-Al_2O_3-TiO_2 melts at 1027 °C takes place in two steps [$Ti^{4+} \rightarrow Ti^{3+} \rightarrow Ti^0$]. Qin et al. (2006)[44] studied the mechanism of Ti^{4+} reduction on graphite electrode and aluminum electrode in Na_3AlF_6-TiO_2 molten salt at 1050 °C by cyclic voltammetry and chronoamperometry. It was found that the reduction of Ti^{4+} on the graphite electrode is a two-step reversible process [$Ti^{4+} \rightarrow Ti^{2+} \rightarrow Ti^0$]. In contrast, the reduction of Ti^{4+} on the aluminum electrode is a one-step process [$Ti^{4+} \rightarrow Ti^0$] due to under-potential deposition. Sun et al. (2008)[45] also concluded from studies by cyclic voltammetry and chronoamperometry that the electrochemical reduction of Ti^{4+} on the tungsten electrode in Na_3AlF_6-AlF_3-TiO_2 melts was a two-step process [$Ti^{4+} \rightarrow Ti^{2+} \rightarrow Ti^0$].

Chloride molten salt electrolysis.—It is interesting to electrodeposit metallic titanium from $TiCl_4$ in molten chloride melts. Table IV shows the various studies on the electrochemical behavior of titanium ion species (such as $TiCl_4$ and $TiCl_3$) in different kinds of chloride melts (e.g., LiCl-KCl, NaCl-KCl, and NaCl-CsCl, etc.).

Chassaing et al. (1981)[47] investigated the electrochemistry of $TiCl_3$ in three molten salts (LiCl, CsCl, and LiCl-KCl) at 700 °C. An Ag/AgCl served as the reference electrode, while a nickel (Ni) wire was used as the working electrode. It was found that the reduction of Ti^{3+} species occurs via two steps [$Ti^{3+} \rightarrow Ti^{2+} \rightarrow Ti^0$] in all three baths. Namely, Ti^{3+} is first reduced to Ti^{2+} at −1.6 V while reducing Ti^{2+} to metal titanium proceed at −2.1 V.

Ferry et al. (1988)[48] studied the electrochemistry of Ti^{2+} in LiCl-KCl eutectic melt by pulse techniques and ac impedance measurements. They concluded that the reduction of Ti^{3+} to Ti^{2+} is quasi reversible, while the deposition of titanium from Ti^{2+} is irreversible. Ferry et al. (1990)[55] also investigated the electrochemical oxidation of Ti^{3+} in LiCl-KCl eutectic melt at 470 °C. They found that Ti^{3+} can be oxidized to soluble Ti^{4+} species at potentials of lower than −0.48 V vs the Ag/AgCl reference electrode.

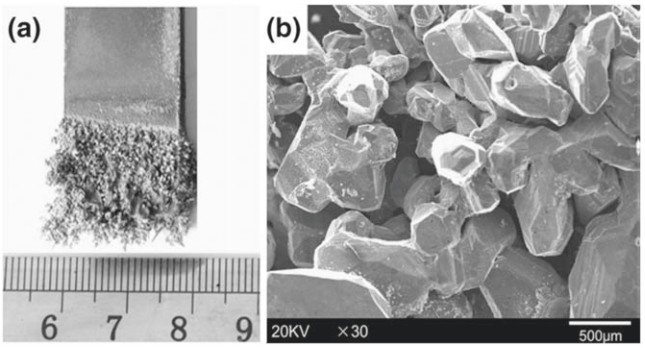

Figure 2. (a) Image of deposited titanium and (b) corresponding morphology obtained under the starting current density of 0.5 A cm^{-2} in $CaCl_2$-$TiCl_2$ (5.0 wt.%) at 1173 K (900 °C).[53]

Chen et al. (1987)[49] investigated the electrochemistry of K_2TiF_6 in NaCl-KCl melts at 700 °C. The Ag/AgCl was used as the reference electrode, while a Pt wire with a diameter of 0.5 mm was used as the working electrode. It was found that the reduction of Ti^{4+} proceeds through a three-step process [$Ti^{4+} \rightarrow Ti^{3+} \rightarrow Ti^{2+} \rightarrow Ti^0$]. The authors (1988)[56] also investigated the electrochemical reduction of K_2TiF_6 in NaCl-KCl melts with the addition of KF. The three-step reduction process was suggested in NaCl-KCl-3wt.%KF melts, while the two-step reduction process [$Ti^{4+} \rightarrow Ti^{3+} \rightarrow Ti^0$] was proposed in NaCl-KCl-10wt.%KF melts. Similar results were reported by Lantelme et al. (1995, 1998),[50,51] who studied the reduction of $TiCl_4$ on a tungsten electrode in NaCl-KCl melts, and Barner et al. (2005).[57]

On the other hand, Ning et al. (2011)[52] investigated the electrochemical behavior of $TiCl_2$ in NaCl-KCl melts at 750 °C using cyclic voltammetry, chronopotentiometry, and square wave voltammetry techniques. The results showed that the reduction of Ti^{2+} on a tungsten wire was a one-step diffusion-controlled process. The increase of current density and titanium ion concentration resulted in the increasing grain size of the deposited titanium.

Kang et al. (2015)[53] reported a new process in that metallic titanium with 0.24 mass% oxygen was produced by electrolysis from $CaCl_2$−5wt.%$TiCl_2$ melt at 900 °C. The results from cyclic voltammetry, chronopotentiometry, and square wave voltammetry studies proved that reducing Ti^{2+} on a glassy carbon electrode was a one-step diffusion-controlled process. In addition, the cathodic current efficiency of titanium deposition ranges from 23.74 to 64.40% at different current densities (0.1–0.9 A cm^{-2}). However, the deposited titanium has dendritic structures, as shown in Fig. 2.

Song et al. (2016)[54] investigated the electrochemical behavior of $TiCl_3$ in NaCl-2CsCl melts at 750 °C using cyclic voltammetry, chronopotentiometry, and square wave voltammetry. The results showed that the reduction of Ti^{3+} on a tungsten wire was an irreversible two-step diffusion-controlled process [$Ti^{3+} \rightarrow Ti^{2+} \rightarrow Ti^0$]. The diffusion coefficient for Ti^{3+} at 750 °C was reported to be 10.8×10^{-5} cm^2 s^{-1}. Metallic titanium was obtained by constant current electrolysis from the melt of NaCl-2CsCl-$TiCl_3$ (2 wt.%).

Table IV. Summary of the electrochemical mechanisms of titanium species in various chloride molten salts.

Molten salts	Working electrode	Reduction mechanism	References
(LiCl, CsCl, LiCl-KCl)-$TiCl_3$	Nickel (Ni)	$Ti^{3+} \rightarrow Ti^{2+} \rightarrow Ti^0$	Chassaing et al. (1981)[47]
LiCl-KCl-$TiCl_3$	Tungsten (W)	$Ti^{3+} \rightarrow Ti^{2+} \rightarrow Ti^0$	Ferry et al. (1988)[48]
NaCl-KCl- K_2TiF_6	Platinum (Pt)	$Ti^{4+} \rightarrow Ti^{3+} \rightarrow Ti^{2+} \rightarrow Ti^0$	Chen et al. (1987)[49]
NaCl-KCl-$TiCl_4$	Tungsten (W)	$Ti^{4+} \rightarrow Ti^{3+} \rightarrow Ti^{2+} \rightarrow Ti^0$	Lantelme et al. (1995, 1998)[50,51]
NaCl-KCl-$TiCl_2$	Tungsten (W)	$Ti^{2+} \rightarrow Ti^0$	Ning et al. (2011)[52]
$CaCl_2$−5wt.%$TiCl_2$	Glass carbon	$Ti^{2+} \rightarrow Ti^0$	Kang et al. (2015)[53]
NaCl-CsCl-$TiCl_3$	Tungsten (W)	$Ti^{3+} \rightarrow Ti^{2+} \rightarrow Ti^0$	Song et al. (2016)[54]

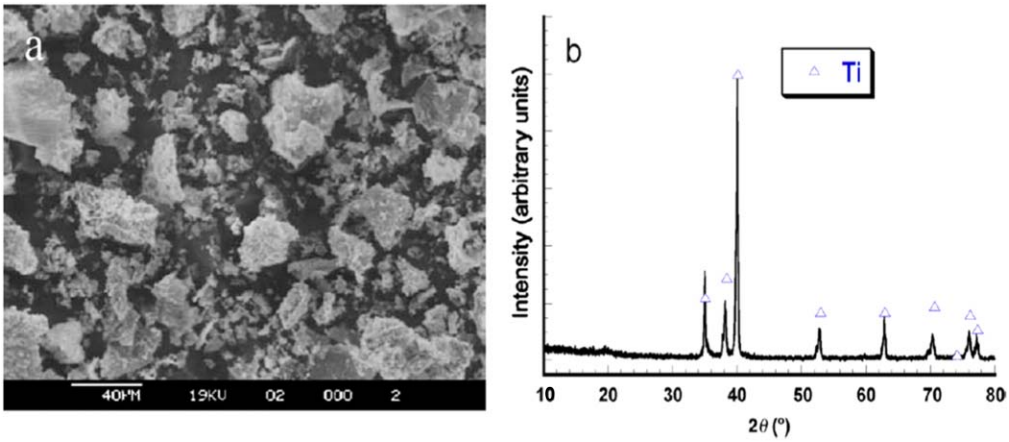

Figure 3. (a) Morphology and (b) XRD pattern of product deposited on the cathode by electrolysis of Ti_2CO solid solution in NaCl–KCl melt.[14]

Zhu et al.[58] developed an exciting titanium production process at the University of Science and Technology Beijing (USTB). In the USTB process, the pellets of Ti_2CO solid solution served as the anode, while carbon steel was applied as the cathode. It was reported by Jiao et al. (2007)[14] that titanium powders with less than 0.3 mass % oxygen were produced by electrolysis in NaCl-KCl molten salt at a temperature of 800 °C and constant potential of −0.45 V vs Ag/AgCl reference electrode. Besides, carbon monoxide (CO) was produced at the anode during electrolysis. As shown in Fig. 3, pure titanium with a grain size of more than 40 μm was found.

Jiao et al. (2010)[59] produced conductive TiC_xO_{1-x} solid solutions by carbothermic reduction of TiO_2 for 4 h at the temperature range of 1500 °C–1700 °C and vacuum of lower than 100 Pa.

When TiC_xO_{1-x} solid solutions were used as the anode, both CO and CO_2 gases are evolved at the anode during electrolysis in NaCl-KCl melts. As shown in Fig. 4, the reactions of the USTB process are given by Eqs. 14 and 15.

$$\text{Cathode reaction: } Ti^{n+} + ne^- \rightarrow Ti \quad [14]$$

$$\text{Anode reaction: } TiC_xO_{1-x} - ne^- \rightarrow Ti^{n+} + yCO + (x-y)CO_2 \quad [15]$$

FFC Process

The Fray-Farthing-Chen (FFC) process, developed by Derek Fray, Tom Farthing, and George Chen at the University of Cambridge in 2000,[12] was evaluated for scale-up and commercial adaption.[60] As shown in Fig. 5, the cathode consisted of solid TiO_2 pellets that were sintered at 800 °C–950 °C in the air to increase their strength, while the graphite was used as an anode in the molten $CaCl_2$ bath. TiO_2 pellets were reduced to titanium metal in the voltage range of 2.8–3.2 V and a temperature range of 850 °C–950 °C. The reactions are given by Eqs. 16 and 17.

$$\text{Cathode Reactions: } TiO_2 + 4e^- \rightarrow Ti(Cathode) + 2O^{2-} \quad [16]$$

$$\text{Anode Reactions: } C + xO^{2-} - 2xe^- \rightarrow CO_x\,(x = 1 \text{ or } 2) \quad [17]$$

Although TiO_2 is usually an insulator, it becomes conducting due to the formation of Magnelli phases (TiO_{2-x}). Meanwhile, the oxygen is ionized, diffused out of the TiO_2 pellets into the $CaCl_2$ melt, and then traveled to the graphite anode, where oxygen anions get discharged to form CO/CO_2.[12] Compared with the conventional Kroll process, the advantages of the FFC process include (i) fewer processing steps, (ii) potential continuous operation, (iii) environmentally more beneficial

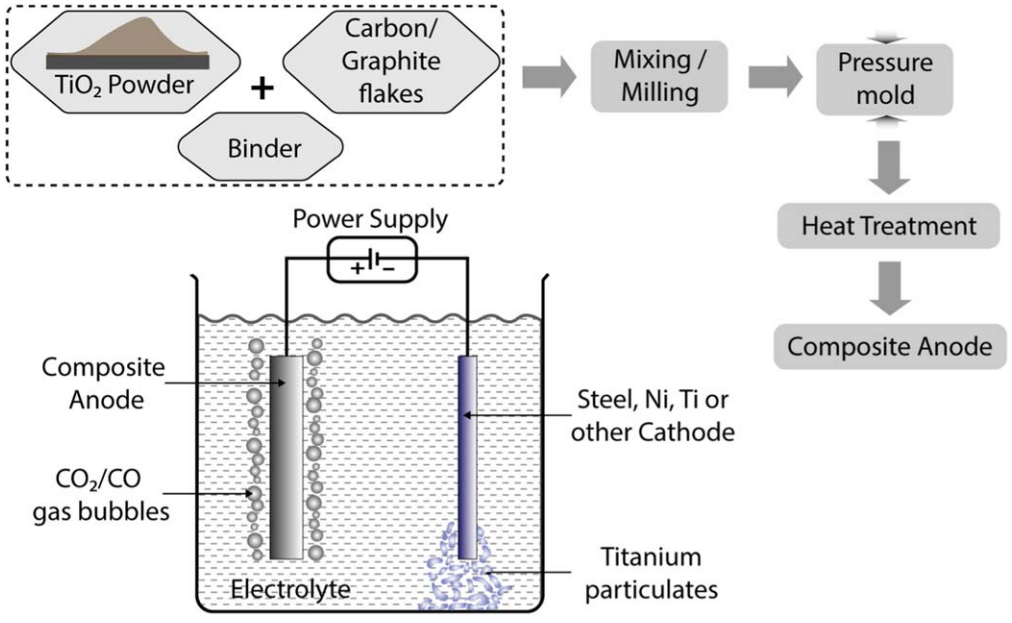

Figure 4. Schematic diagram of the USTB process.[58]

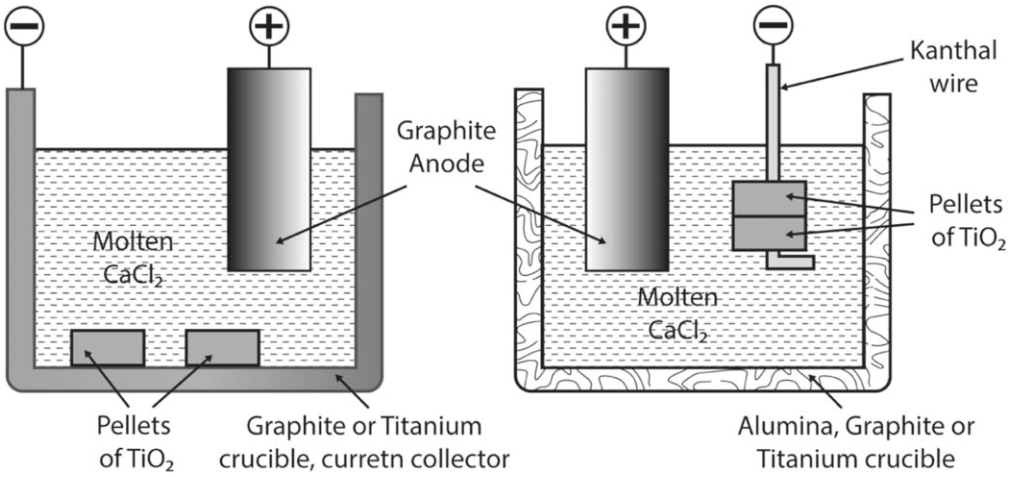

Figure 5. Schematic illustration of the Fray-Farthing-Chen (FFC) process.[12]

due to the use of $CaCl_2$ molten salt instead of chlorine gas, (iv) low oxygen content (<1000 ppm) of the produced titanium.[61] However, this process's disadvantages are slow oxygen diffusion, low current efficiency, and titanium separation from the waste $CaCl_2$ melts after electrolysis. FFC process has shown acceptable energy consumption of 33 kWh kg^{-1} Ti but it suffers from very low current efficiency (15%) to produce Ti with low oxygen content (~0.3 wt% O).[62]

Chen et al. (2002)[63] studied the electrochemical behavior of oxide-scale-coated titanium electrodes in pre-electrolyzed (2.7–3.0 V) molten $CaCl_2$ at 900 °C by cyclic voltammetry. According to three reduction peaks at electrode potentials more positive than the reduction of Ca^{2+}, they suggested that the reduction of solid TiO_2 to titanium involved three steps: $TiO_2 \rightarrow Ti_2O_3 \rightarrow TiO \rightarrow Ti^0$. However, Wang et al. (2004)[64] concluded from studies by cyclic voltammetry, chronoamperometry, and ac impedance techniques suggesting that titanium was produced by a two-step process reduction of solid TiO_2 ([$TiO_2 \rightarrow TiO \rightarrow Ti^0$]) in molten $CaCl_2$ at 800 °C–900 °C. Similar results were observed by Nie et al. (2006).[9] They concluded that the reduction of TiO_2 to titanium was a two-step process ([$TiO_2 \rightarrow TiO \rightarrow Ti^0$]), and the application of different cell voltages at different stages can improve the current efficiency.

Dring et al. (2005)[65] studied the mechanism of cathodic deoxygenation of TiO_2 in molten $CaCl_2$ at 900 °C. Based on cyclic voltammetry study and characterization of TiO_2 working electrode, the deoxygenation of TiO_2 to Ti_3O_5 and Ti_2O_3 occurs at the potential of 300 mV more negative than the TiO_2 open-circuit potential, while the decomposition of the Ti_2O_3 to TiO and metallic titanium proceeds at potentials 1100 mV more negative. Thus, the deoxygenation of TiO_2 in molten $CaCl_2$ at 900 °C proceed by four steps ([$TiO_2 \rightarrow Ti_3O_5 \rightarrow Ti_2O_3 \rightarrow TiO \rightarrow Ti^0$]). Similar results were reported by Wang et al. (2011)[66] in molten $CaCl_2$ at 950 °C. Schwandt et al. (2005)[67] and Alexander et al. (2011)[68] investigated the kinetic pathway in the electrochemical reduction of TiO_2 in molten $CaCl_2$. Based on the X-ray diffraction analysis of cathodic samples at deferent electrolysis time (0.5, 1, 4, 12, 52, and 120 h), the reduction (at 2.5 V) process proceeds via a number of individual stages: $TiO_2 \rightarrow Ti_4O_7 + CaTiO_3 \rightarrow Ti_3O_5 + CaTiO_3 \rightarrow Ti_2O_3 + CaTiO_3 \rightarrow TiO + CaTiO_3 \rightarrow CaTi_2O_4 \rightarrow Ti^0$.

Wang et al. (2006)[69] attempted to obtain titanium from cheap TiO_2 feed material (including titania dust, meta-titanic acid, and titanium-rich slag) by the FFC process. Low-cost TiO_2 precursors help reduce the cost of commercial application of the FFC process. Titanium with low oxygen content (<3000ppm) was obtained by constant voltage electrolysis (2.9–3.1 V) at 900 °C in molten $CaCl_2$. Besides, they reported that the current efficiency was dependent on the electrolysis time and the pellet thickness. For TiO_2 pellets with a thickness of 2 mm, the current efficiency decreases from 40% in the first 5 h to 20% in 12 h. The energy consumption of 12 h electrolysis was 33 kWh kg^{-1} Ti, which was less than the conventional Kroll process (50 kWh kg^{-1} Ti).[61] According to their discussion, energy waste mainly came from the background current (20 kWh kg^{-1} Ti).

Liu et al. (2007)[70] investigated the electrolysis voltage effect and reported that the optimized cell voltage for electrolysis of solid TiO_2 in molten $CaCl_2$ was 2.6–3.1 V. When the voltage of 1.5–1.7 V was applied, Ti_2O was reduced to Ti_3O because of oxygen ionization, but no titanium was detected. When higher voltages (2.1–3.1 V) were applied, TiO_2 and Ti_2O were reduced to metal titanium. Besides, they found that the oxygen content decreases rapidly at the voltage of 2.1–2.6 V and then shows little change at 2.6–3.1 V. According to their discussion, voltages for electrolysis should be determined by the decomposition voltage of both CaO (2.6 V) and $CaCl_2$ (3.2–3.3 V). A similar study was performed by other researchers.[71]

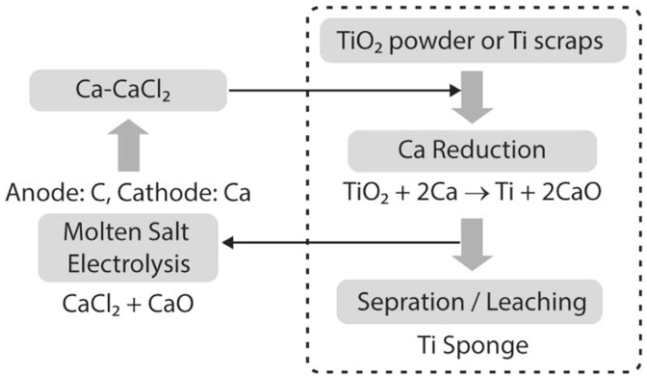

Figure 6. Schematic illustration of the OS process.[13]

The OS process (Calciothermic Reduction)

Ono and Suzuki developed the Ono and Suzuki (OS) process from Kyoto University, as illustrated in Fig. 6.[13] They proposed calcium (Ca) as the reductant to reduce TiO_2 powder to metal titanium, and calcium is continuously formed from the electrolysis of the by-product CaO in the $CaCl_2$ molten salts. At 3.0 V, higher than the decomposition voltage of CaO (1.66 V) but below that of $CaCl_2$ (3.2 V), liquid calcium gets deposited on the cathode, while both CO_2 and CO gases are emitted from the carbon anode. Therefore, the main reactions of the OS process are given by Eqs. 18–20.

$$\text{Cathode reactions: } CaO + 2e^- \rightarrow Ca + 2O^{2-} \quad [18]$$

Anode reactions: $C + xO^{2-} - 2xe^{-} \rightarrow CO_x\ (x = 1\ or\ 2)$ [19]

Calciothermic reduction reaction: $TiO_2 + 2Ca \rightarrow Ti + 2CaO$ [20]

In comparison to the FFC process, the composition of molten salts ($CaCl_2$), the carbon anode, and the applied voltage are similar, but the operating mechanisms are different. The sintered TiO_2 pellets were used as the cathode in the FFC process, and oxygen diffusion in the titanium cathode was required. However, TiO_2 does not need to contact the cathodic lead in the OS process, and it can be fed in powder form. Besides, the OS process suggested that TiO_2 was reduced to titanium by Ca, and it is a short-term reduction and de-oxidation process without the requirement of oxygen diffusion in a long distance.

Suzuki et al. (2003)[72] found that when pure calcium (Ca, 5–7 mol%) coexisted with $CaCl_2$ molten salts at 900 °C, TiO_2 was successfully reduced to metallic Ti powder with less than 0.1 mass% oxygen and 0.15 mass% Ca only for 3600 s.

As an extension of the OS process, Suzuki et al. (2003)[73] combined both the calciothermic reduction and the in situ electrolysis of CaO in the CaO-$CaCl_2$ molten salt at 900 °C using carbon anode and Ti basket-type net cathode (filled with TiO_2 Powder). They conducted that the optimal concentration of CaO in the $CaCl_2$ melt was 0.5–1 mol% because α-Ti single phase could be obtained only from salts with a lower concentration of CaO. A metallic titanium sponge with 0.2 mass% oxygen was produced at the voltages ranging from 2.6–2.9 V for 10800 s in 0.5 mol% CaO-$CaCl_2$ melts. However, the current efficiency of the OS process was low (8.8%–25.5%) because of parasitic reactions and back reactions.

Suzuki et al. (2004)[74] also investigated Ca distribution in the CaO-$CaCl_2$ molten bath during electrolysis, and experiments were carried out with different positions of TiO_2 samples. When TiO_2 samples were placed in the cathode's close vicinity, α-Ti with 0.16 mass% oxygen was produced. However, TiO_2 was partially reduced to lower valence oxides such as Ti_2O_3, TiO, or Ti_2O when TiO_2 samples were placed separated from the cathode. The authors (2005)[75] also tried stirring the melt to accelerate the reaction, but they found that stirring lowered the Ca concentration on the cathode surface, and the reduction of TiO_2 was incomplete.

To obtain lower oxygen content in titanium by the reduction of TiO_2 in CaO-$CaCl_2$ molten salt, Kobayashi et al.[76] studied the influence of current density and electrode distance. It was found that α-Ti with 0.08 mass% oxygen was produced when the cathodic current density was high, and a 15 mm basket with a sufficiently large inner capacity was used as a cathode.

Imam et al.[77] have described the developments on cost-effective approaches to fabricate titanium components under various aspects of powder metallurgical technology. The factors discussed include blended elemental approach, pre-alloyed techniques, additive layer manufacturing, metal injection molding, spray deposition, and microwave sintering. In addition, a brief review of low-cost powder production processes such as the FFC Cambridge, MER, commonwealth scientific and industrial research organization (CSIRO) method, and ITP/Armstrong are presented. Some of these methods are discussed in this article. Armstrong process technology and CSIRO's direct powder rolling (DPR) and hot roll densification (HRD) processes are found to be useful methods of processing titanium powder into consolidated parts, and sheets are reported.[78]

Bogala and Reddy[79] performed a thermodynamic assessment of the electrochemical reduction of TiO2 to Ti metal in $CaCl_2$ molten salt electrolyte using the FFC process. The conversion of TiO_2 to Ti takes place via multi-step reduction processes that involve the formation of several intermediates or sub-oxides of titanium at different reaction conditions. This research article discusses the thermodynamic modeling studies on the formation of varying titanium sub-oxides and corresponding reaction conditions such as a change in Gibbs energy, temperature, and pressure during TiO_2 reduction to Ti metal. Figure 7 shows the comparison of calculated changes in Gibbs energy of calciothermic reduction of titanium sub-oxides with experimental standard values from literature at 1000, 1100, and 1200 K. The negative changes in the Gibbs energy values suggest that all the reactions are exothermic (occur spontaneously in the forward direction). The reduction of TiO_2 to Ti occurs via CaO or/and Ca mediated pathway ($TiO_2 \rightarrow Ti_nO_{2n-1} \rightarrow Ti_3O_5 \rightarrow Ti_2O_3 \rightarrow TiO \rightarrow Ti_3O_2 \rightarrow Ti$). Ti metal oxidation to TiO_2 occurs through CO_2 or/and CO mediated pathway ($Ti \rightarrow Ti_3O_2 \rightarrow TiO \rightarrow Ti_2O_3 \rightarrow Ti_3O_5 \rightarrow Ti_nO_{2n-1} \rightarrow TiO_2$). The titanates ($CaTiO_3$, $CaTi_3O_7$, $Ca_2Ti_2O_5$, $Ca_3Ti_2O_6$, $Ca_3Ti_2O_7$, and $Ca_5Ti_4O_{13}$), carbides (TiC and CaC_2), C, CaO, and chlorides ($TiCl_4$ and $CaOCl_2$) were identified as additional stable species at 1,200 K and 1 bar.

PRP method and EMR method

The Preform Reduction Process (PRP) illustrated in Fig. 8 was developed by Okabe et al. (2004) from the University of Tokyo.[80] They used the concept of calciothermic reduction to produce titanium from TiO_2, like the OS process that uses $CaCl_2$ or CaO-$CaCl_2$ melts as a flux to facilitate the reduction. However, the PRP method is a metallothermic reduction process without the electrolysis of CaO. The calcium vapor was applied to react with preforms, which were made by sintering the mixture of TiO_2 powder, flux (such as $CaCl_2$ or CaO), and binder (such as collodion, which is a mixture of 5 mass% nitrocellulose in ethanol and ether) at 800 °C. The sintered preforms and reductant Ca were placed in a stainless-steel vessel at a constant temperature ranging from 800 °C to 1000 °C for 6 h. After leaching the reduced preforms by acid, titanium powder with a purity of 99 mass% was obtained. The advantages of this process are the ability to control the purity and produce homogeneous fine titanium powder. However, the PRP method still has some drawbacks, such as the expensive cost of reductant Ca.

Jia et al.[81] obtained Ti powders by calcium vapor reduction of TiO_2 directly through the formation of an essential intermediate $CaTiO_3$ compound. It was stated that based on thermodynamic calculation, the Gibbs energy change of the reaction to produce $CaTiO_3$ by CaO and TiO_2 is always negative below 1000 °C. The Gibbs energy change of the calciothermic reduction reaction of $CaTiO_3$ is lower than that of TiO, which is the most predominant step to convert TiO_2 to Ti. The experiments suggested that the $CaTiO_3$ phase was derived from the reaction between TiO_2 and the reduction by-product CaO resulting from the calcium vapor reduction process of titanium oxide. However, $CaTiO_3$ could be reduced to Ti much easier than that of TiO_2 by using calcium vapor. So, the experimental conditions are equally beneficial for the formation of intermediate $CaTiO_3$ as wells as for preparing Ti via TiO_2 reduction by calcium vapor.

The electronically mediated reactions (EMR) was developed by Park et al. at the University of Tokyo.[82] The EMR process provides an effective method to control the location and morphology of the metal deposits. The process produces Ti powder directly from TiO_2 by using calcium as a reductant. Feed material (TiO_2 powder or preform) and reductant (Ca–Ni alloy) were charged in electronically isolated locations in a molten calcium chloride ($CaCl_2$) salt at 1173 K, and the current flow through an external circuit between the feed and reductant locations was monitored during the reduction of TiO_2. The voltage between the feed electrode and reductant alloy was intermittently measured during the reduction experiment to monitor the reduction process. After the reduction experiment, pure titanium powder with low nickel content was obtained even though liquid Ca–Ni alloy was used as a reductant. The EMR process produces titanium of high purity (99.5 mass%). Okabe and Waseda[83] have also elaborated on the EMR process. Figure 9 schematically shows the comparison of conventional magnesiothermic and EMR

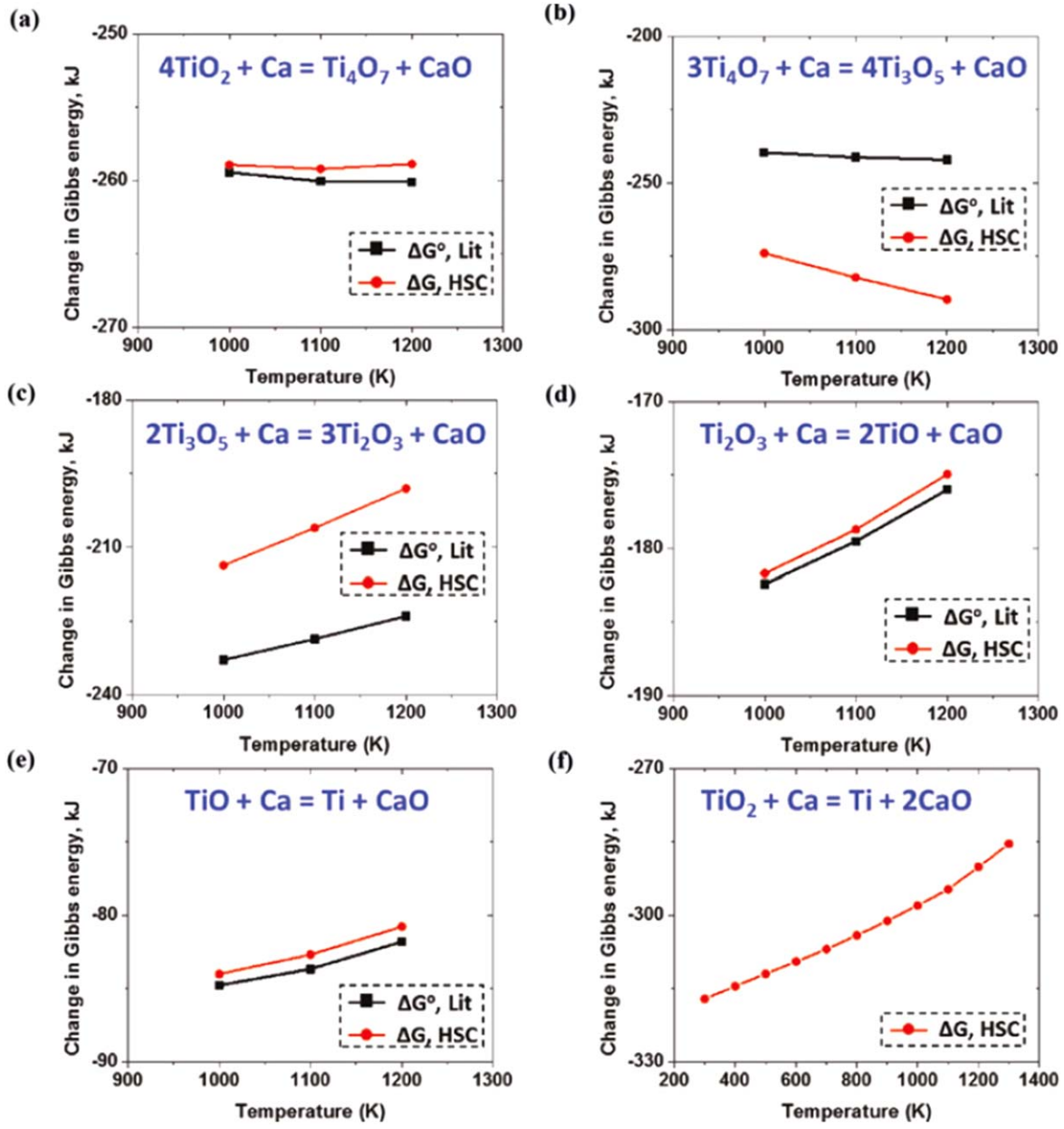

Figure 7. Change in Gibbs energy for calciothermic reduction of Ti oxides at 1000–1200 K.[79]

methods for the reduction of $TiCl_4$. Metallothermic reduction aims to produce the desired metal by reducing the metal from compounds using a metallic reductant. The process, often accompanied by heat evolution, is widely used for producing metals such as titanium and tantalum (Fig. 9a).[84] Here, the reduction of $TiCl_4$ by magnesium occurs by direct physical contact between the reactants. On the contrary, the conventional reaction in Fig. 9a can be divided into two reactions (Fig. 9b) to occur at two different sites when an electrically conducting medium exits to facilitate electron transfer and local electro-neutrality conditions are satisfied.

Armstrong Process

The Armstrong Process® technology produces Ti powder by injecting titanium tetrachloride ($TiCl_4$) in vapor form into a flowing stream of liquid sodium. The metal chlorides react with the sodium to leave the pure metal, with sodium chloride being generated as a by-product (Fig. 10a). In the Armstrong process, the powder is made as a product of extractive processes that produce the primary metal powder. Such an approach can produce commercially pure Ti (CP-Ti) powder by $TiCl_4$ and other metal halides using sodium (Na).[85] The produced powder particles possess unique properties and low bulk density. Additional post-processing activities such as dry and wet ball milling are applied to further improve the particle size distribution and the tap density of the powder. Besides, the powder's morphology produced by the Armstrong process provides for excellent compressibility and compactness. Figure 10b shows the scanning electron microscopy (SEM) image of the CP-Ti powder produced by the Armstrong process. The SEM image reveals that the powder synthesized using the Armstrong process has an irregular morphology made of granular agglomerates of smaller particles.

The Hydride-Dehydride (HDH) Process

Figure 11a depicts the hydride-dehydride (HDH) process, which can produce Ti powder using Ti sponge, Ti mill products, or Ti scrap as the raw material.[86,87] The hydrogenation process is achieved utilizing a batch furnace that usually operates in a vacuum and/or atmospheric

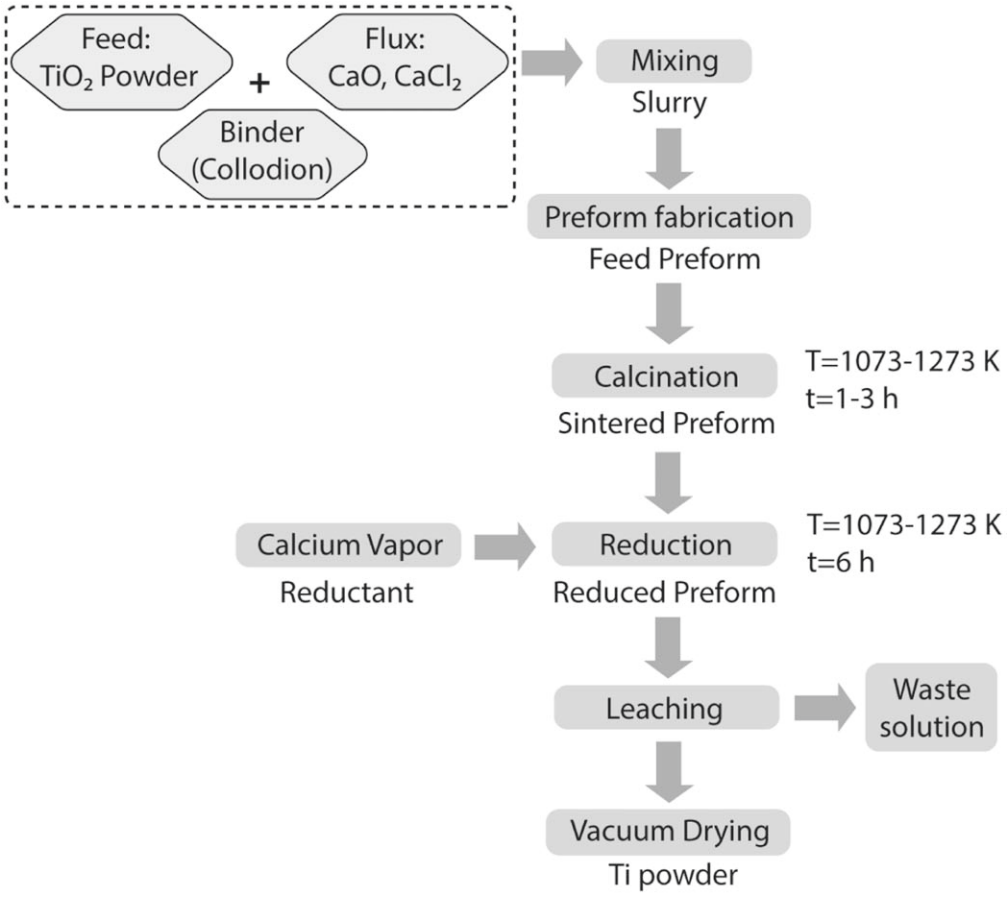

Figure 8. Flowchart of titanium powder production using preform reduction process (PRP).[80]

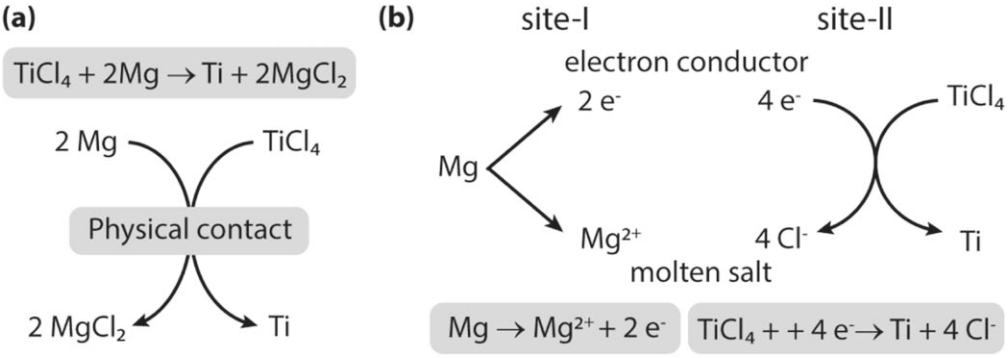

Figure 9. Schematic illustration of the reduction of $TiCl_4$ via (a) conventional magnesio-thermic process and (b) EMR process.[82]

hydrogen conditions. The hydrogenation conditions of titanium are the pressure of one atmospheric and temperatures of utmost 800 °C.

HDH process produces titanium hydride and alloy hydrides that are usually brittle, which can be milled and screened to make fine powder particles. The powder is resized using various powder-crushing and milling techniques such as a jaw crusher, ball milling, or jet milling. Upon crushing and classifying, the titanium hydride powders are put back in the batch furnace to dehydrogenate and remove the interstitial hydrogen under a vacuum or argon atmosphere to finally produce the metal powder. These powders are irregular and angular in morphology and can also be magnetically screened and acid-washed to remove any ferromagnetic contamination (Fig. 11b). The powder could be passivated upon completion of the hydrogenating and dehydrogenating cycles to minimize exothermic heat generated upon exposure to the air. Such an HDH process is relatively inexpensive due to the lower cost of the hydrogenation and dehydrogenation processes. Moreover, the purity of the powder obtained can be very high if the raw material's impurities are reduced. The final powder's oxygen content strongly depends on the input material, the handling processes, and the specific surface area of the powder. Therefore, the main demerits of HDH powder include irregular powder morphology. The process is not suitable for making virgin-alloyed powders or modifying alloy compositions if the raw material is from scrap alloys.

Multi-arc Fluidized Bed Reactor (MAFBR) Process

SRI International has developed a new way of producing titanium powder in fewer steps and is less energy-intensive than conventional methods (Fig. 12).

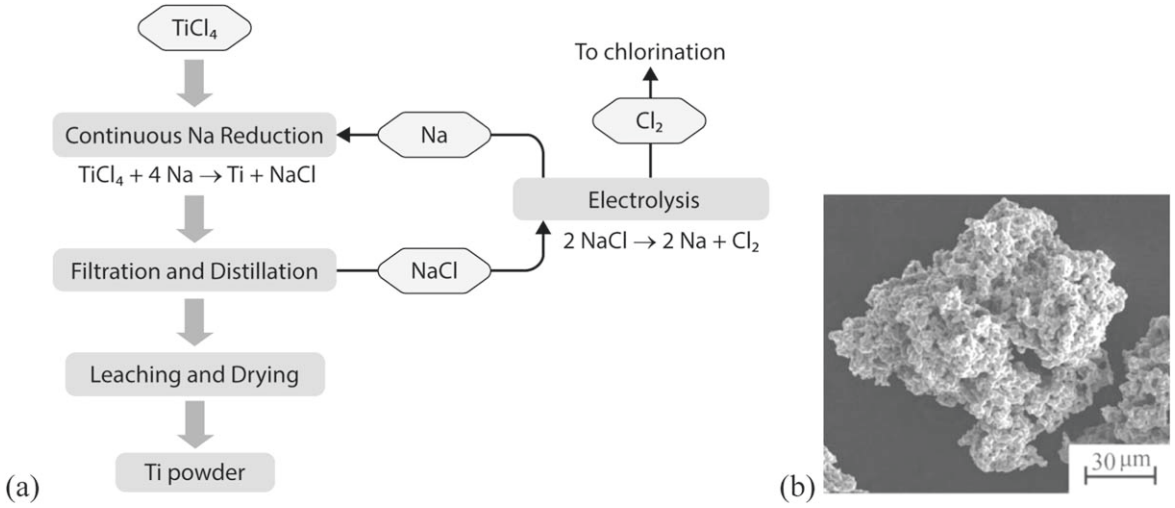

Figure 10. (a) Schematic illustration of the Armstrong process, (b) SEM micrograph of CP-Ti produced by Armstrong process.[85]

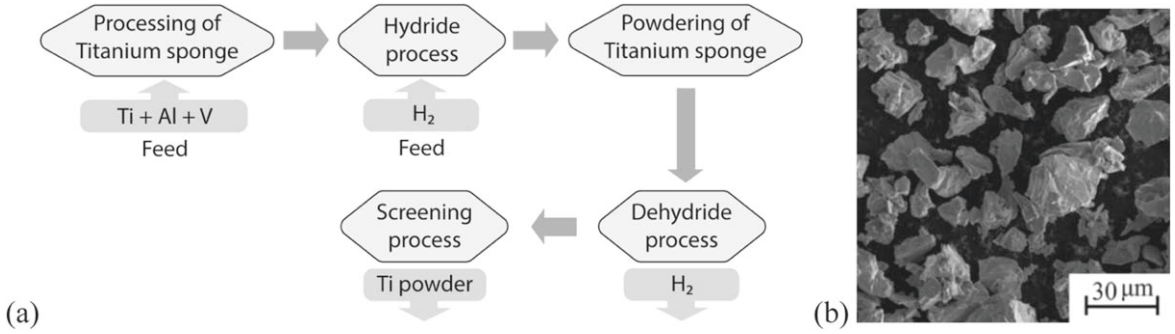

Figure 11. (a) Hydride-dehydride (HDH) process for the production of titanium powder.[86]

SRI's process utilizes plasma arcs to facilitate reactions between hydrogen and titanium chloride ($TiCl_4$), a chemical produced from titanium ore. Like lightning bolts, arcs crack the hydrogen, producing atomic hydrogen that can readily react and produces titanium vapor that rapidly solidifies and forms a titanium powder.[88] The synthesized powder could be pressed into the required shape and size, thereby reducing the amount of machining required. The SRI has so far demonstrated a small-scale version of the process for producing pure titanium. It's currently working on a two-stage approach to improve yields and lower costs before scaling it up. The advantages of such process include the production of granules that are ready to be used in powder metallurgy (particle sizes from 10 s of microns to mm), use of atomic hydrogen as reducing agent, direct production of alloys, and the process could apply to other metals, ceramics as well. However, the only limitation of this process is that the $TiCl_4$ undergoes disproportionation reactions by which it forms $TiCl_2$ solid particles, which are at times hard to reduce.

The CSIRO has developed a similar methodology using the TIRO™ process for continuous, direct titanium powder production.[89] The TIRO process comprises two stages, as shown in Fig. 13a. The first stage is a well-known fluidized bed reactor (FBR) in which $TiCl_4$ is reacted with Mg powder to form solid magnesium chloride particles (~350 μm in diameter) dispersed with micron-sized titanium particles (~1–2 μm in diameter). A continuous vacuum distillation operation is the second stage, where the Ti is separated from the $MgCl_2$ and then sintered to form a friable "biscuit." The biscuit comprises porous titanium spheres about 250 μm in diameter, which can be separated by very light grinding. The overall process yields a throughput of 0.2 kg h^{-1} Ti, meets the CP2 purity specifications with $\leqslant$0.25 wt% O and $<$ 200 ppm Cl. Ring milling of vacuum distilled products can further reduce titanium's particle size (Fig. 13b); however, it can result in the introduction of oxygen if done in the air.

Aluminothermic Reduction Process

A novel approach of two-stage aluminothermic reduction is introduced in a laboratory-scale method to prepare the Ti-6Al-4V powder using Na_2TiF_6 and Al-V alloy as raw materials is reported.[90] The preparation mechanism suggests that the aluminothermic reduction of Na_2TiF_6 is a stepwise reduction process wherein vanadium does not take part in the reduction reaction. Some Ti sub-fluorides and Al sub-fluorides are also generated during the reduction process. Spherical or near-spherical Ti-6Al-4V alloy with uniform distribution of aluminum and vanadium can be obtained after the reduction process and ball milling process. The two-stage aluminothermic reduction reaction occurs with a mass ratio of 1:1 between titanium-containing cryolite and aluminum to produce the powder at a reduction temperature of 1050 °C and a holding time of 30 min. The pure cryolite and Al–Ti alloy powder is obtained at the second aluminothermic reduction stage. The Ti in Ti-containing cryolite is mainly in the form of Na_3TiF_3 with 3% content. Spherical or near-spherical Ti-6Al-4V alloy with uniform distribution of aluminum and vanadium are obtained upon ball milling. The first-stage main reaction proceeds as follows:

$$3Na_2TiF_6 + nNaF + 4Al = 3Ti + (6 + n)NaF + 4AlF_3 \quad [21]$$

The essence of aluminothermic reduction of Na_2TiF_6 is the reaction of Al with TiF_4 to form AlF_3, and the reaction is a stepwise reduction process. The general reactions of Ti synthesis are:

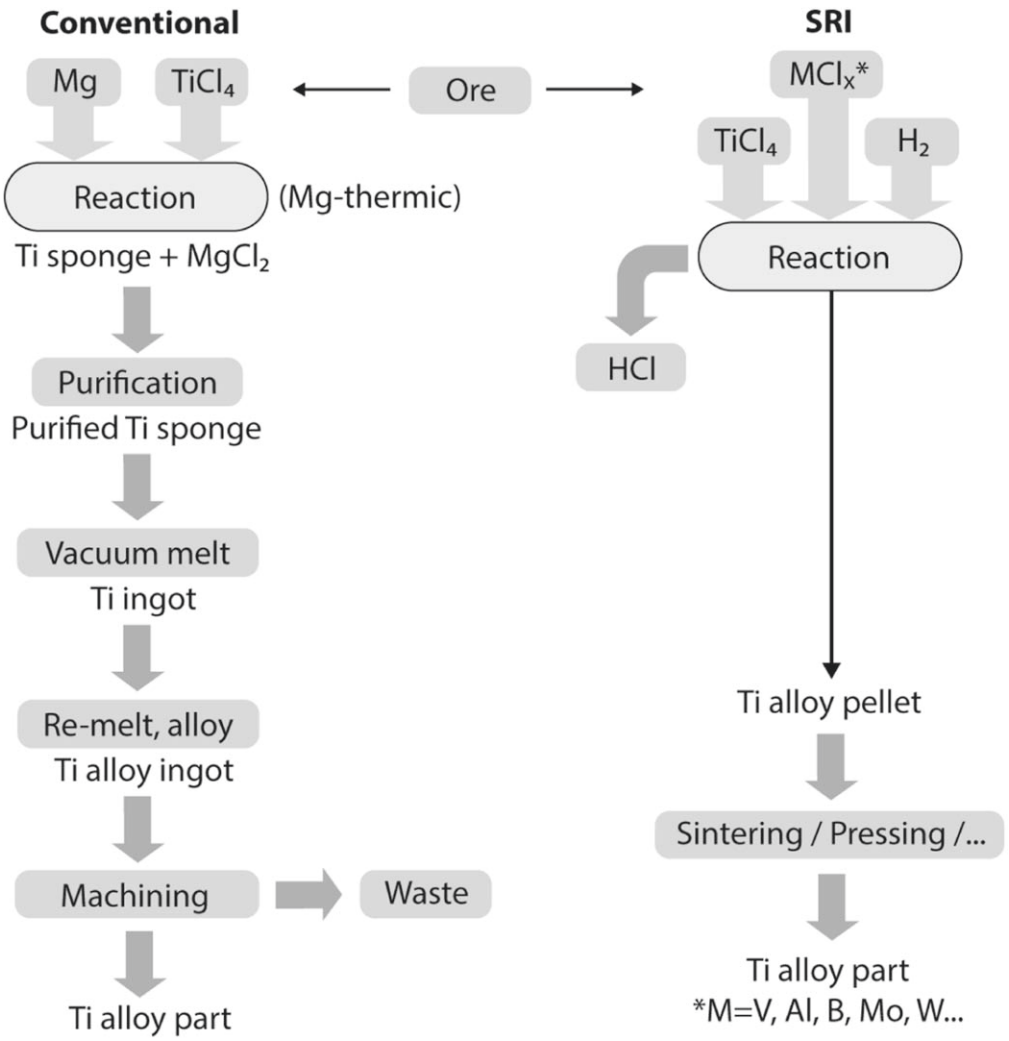

Figure 12. Schematic of multi-arc fluidized bed reactor (MAFBR) process to produce titanium powder by solidification of plasma arc-produced titanium vapor.[88]

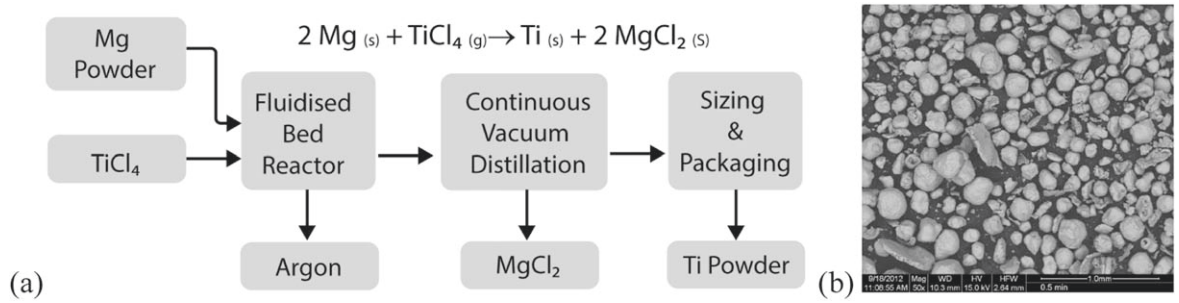

Figure 13. (a) Schematic of TIRO™ process for continuous, direct production of Ti powder and (b) SEM micrographs of TiRO™ powder ring milled for 0.5 min.[89]

$$3Na_2TiF_6 + 6NaF + Al = 3Na_3TiF_6 + Na_3AlF_6 \quad [22]$$

$$Na_3TiF_6 + Al = Ti + Na_3AlF_6 \quad [23]$$

Low-cost production of titanium alloy powder can also be accomplished by a combination of one or more processes.[78,91,92,79] For instance, low-cost Ti-6Al-4V powder can be obtained via (i) one step melting of sponge/alloying and gas blowing alloy powder, (ii) metallothermic reduction of mixed chloride precursors to produce alloy powder, and (iii) electrolytic reduction in a fused salt of mixed alloying ($TiCl_4$-$AlCl_3$-VCl_4) chlorides. The demand to produce such low-cost titanium alloys is growing over the past few years for biomedical applications.[5]

TiPro Process of Producing Low-Cost Ti-Alloy

To reduce the cost of producing titanium alloys, the TiPro process was developed at the University of Waikato by using a

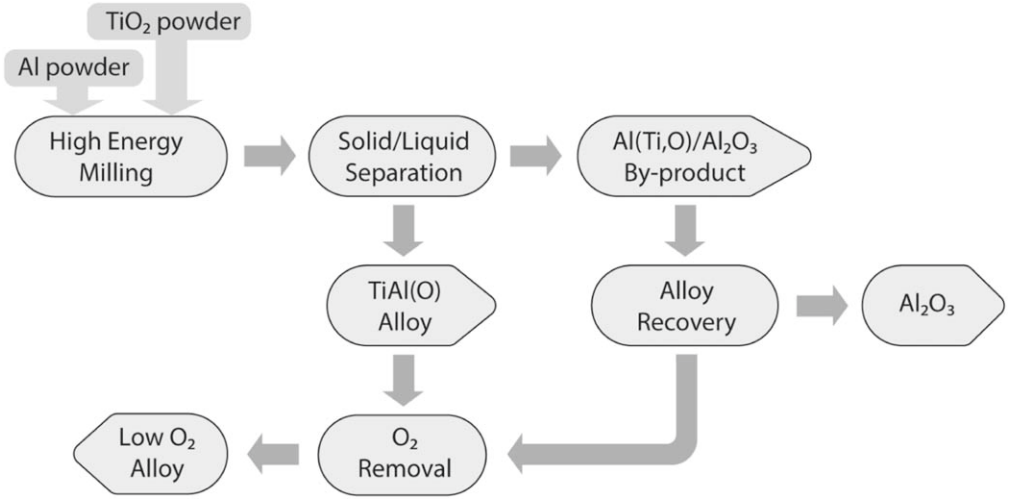

Figure 14. Flowchart of the TiPro process.[93,94]

combination of a combustion synthesis (CS) reaction between low-cost inputs (TiO_2 and Al) and extrusion of the CS product to separate the liquid Ti-Al alloy in a single step.

The use of CS reactions has favorable cost reduction advantages compared to conventional processing because of lower power input, simplicity, short reaction time, and self-cleaning of the combustion product resulting from the volatilization of impurities at the high reaction temperatures. To produce Ti alloy powders, Al/TiO_2 powder mixtures were mechanically activated. The resultant composite powder was subsequently preheated to ignite a combustion synthesis reaction and separate the liquid Ti-Al alloy by extrusion.[93,94] Figure 14 shows the flow diagram of the TiPro process. The reaction of TiPro process is given as Eq. 24:

$$3TiO_2 + 7Al = 3TiAl + 2Al_2O_3 (= -472.37\ kJ) \quad [24]$$

Low-Temperature Reduction Using MgH_2

Low-cost titanium powder can be obtained by producing titanium hydride (TiH_2) powder followed by its transformation to Ti powder through the dehydrogenation process. This method is advantageous as it is possible to provide low oxygen content Ti for powder metallurgy. The typical process involves the reduction of titanium tetrachloride ($TiCl_4$) to TiH_2 with magnesium hydride (MgH_2) under a hydrogen atmosphere.[95] The energy consumption of the process is minimized by setting up the temperature range between 400 °C and 500 °C. The $TiCl_4$ reduction process is carried out by two different methods, as shown in Fig. 15. In the first method, MgH_2 is placed in the crucible in the furnace. Then a stoichiometric amount (from Eq. 25) of $TiCl_4$ is injected into the MgH_2 crucible after 1 h H_2 purging (Fig. 15a).

$$TiCl_{4(g)} + 2\,MgH_2 = TiH_2 + 2\,MgCl_2 + H_{2(g)} \quad [25]$$

$$\Delta G^\circ = -495.920 + 0.065\,T(kJ\ mol^{-1})$$

$$TiH_{2(g)} + 5\,TiCl_{4(g)} = 6\,TiCl_3 + 2\,HCl_{(g)} \quad [26]$$

$$\Delta G^\circ = -382.330 + 0.487\,T(kJ\ mol^{-1})$$

The samples were reduced at 400 °C at different times. The H_2 gas flow rate in this method was set to 100 c.c./min only to ensure STP conditions inside the furnace and prevent the reverse flow of hydrochloride acid (HCl) into the furnace. In the second method (Fig. 15b), H_2 gas is used as a carrier of $TiCl_4$ gas into the furnace. A higher flow rate of H_2 gas is required to ensure enough $TiCl_4$ inside the furnace. The dry H_2 gas is purged into the $TiCl_4$ vessel, heated up to 140 °C to transform into a gaseous state. A mixture of $TiCl_4$ and H_2 gases are transported into the furnace to react with the MgH_2 powder at a specified temperature (400, 450, and 500 °C) and a reaction time of 6 h. The MgH_2 powder is ball-milled for 60 min with 10 wt.% TiH_2 at 400 RPM, and the volume ratio of ball to powder equaled 40. To prevent the excess emission of the $TiCl_4$ gas

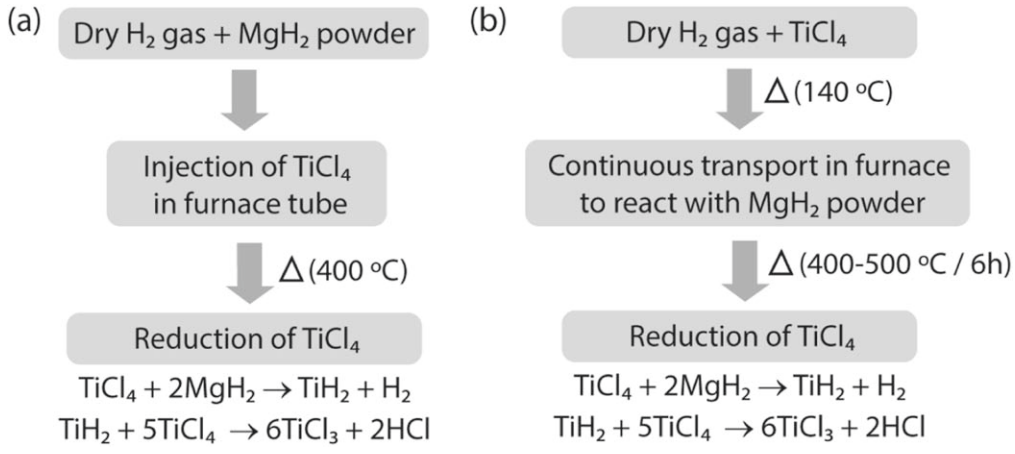

Figure 15. Schematic process: (a) $TiCl_4$ injection method, (b) $TiCl_4$ continuous flow method.[95]

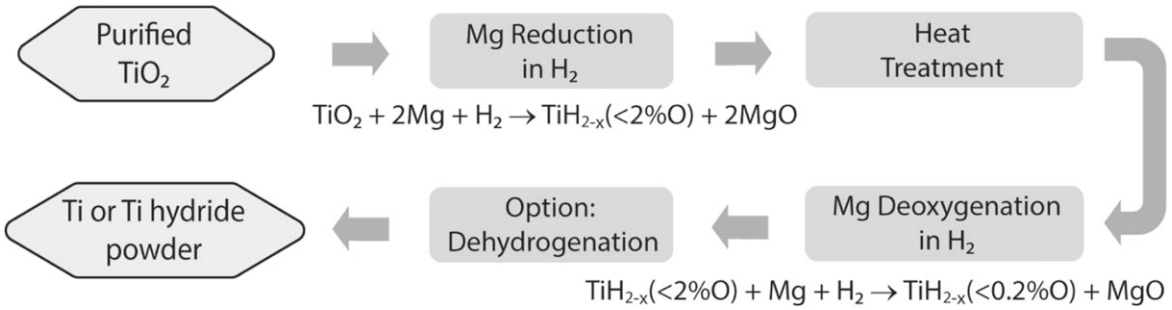

Figure 16. Schematic illustration of main processing steps of the HAMR process.[96,97]

into the atmosphere, a residual exit gas was passed through the HCl bottle to dissolve the extra gas and further neutralized by NaOH solution before it is vented in the atmosphere.

Hydrogen-Assisted Magnesium Reduction (HAMR) Process

A low-cost method based on alkaline roasting at relatively low temperatures followed by a hydrolysis process is used to produce highly purified TiO_2. Such a two-step method is known as the hydrogen-assisted magnesium reduction (HAMR) process, whose main processing steps are illustrated in Fig. 16.[96,97] HAMR process employs a deoxygenation step to ensure sufficiently low oxygen content (< 0.15 wt.) in the final product powder. For this purpose, the HAMR process is designed to include the following three key elements such as the use of hydrogen atmosphere, the use of molten salt, and the adaptation of a two-step process consisting of the main reduction step and a deoxygenation step. Hydrogen helps to destabilize the Ti–O system, increasing the thermodynamic driving force for Mg to react with Ti–O.[98] Additionally, hydrogen is also beneficial to form titanium hydride (TiH_2) instead of Ti metal during the reduction process. TiH_2 is less prone to oxidation in the air compared to α-Ti, which makes it easier to handle the material after reduction and control the oxygen content in the final product. HAMR process has relatively less energy consumption of 58.76 kWh kg^{-1} than the Kroll process.[17] However, it is still considered to be high.

Low-Temperature Molten Salts Electrolysis-Ionic Liquids

Apart from the above high-temperature molten electrolysis process, the electrodeposition of titanium and Al-Ti alloy was reported in chloroaluminate ionic liquids because of their unique chemical-physical properties such as low melting points, high thermal stabilities, negligible vapor pressure, wide electrochemical windows, and high conductivities.

A unique and versatile feature of room temperature chloroaluminate (RTC) ionic liquids is their adjustable chloro-acidity, which can be controlled by the $AlCl_3$ mole fraction (X_{Al}) or the molar ratio of organic chloride salt to $AlCl_3$. Karpinski et al.[99] reported that different chloroaluminate anions such as $AlCl_4^-$, $Al_2Cl_7^-$ and $Al_3Cl_{10}^-$ were formed by changing the mole fraction of $AlCl_3$ in such ionic liquids (BmimCl/EmimCl). In addition, this thermodynamic distribution of Al species in such ionic liquids has been proved experimentally determined by Raman spectroscopy studies.[100,101] RTC ionic liquids can be classified as acidic, neutral, and basic, depending on the $AlCl_3$ content. If $AlCl_3$ content is less ($X_{Al} < 0.5$), the electrolyte contains $AlCl_4^-$ and Cl^- moieties and possess Lewis basic characteristics due to excess unbound chloride ions, whereas, with higher $AlCl_3$ ($X_{Al} > 0.5$), the electrolytes are based on the presence of $AlCl_4^-$ and $Al_2Cl_7^-$ species and have Lewis acidic properties mainly due to coordinately unsaturated $Al_2Cl_7^-$ species. Acidic RTCs are of interest as electrolytes for the electroplating of aluminum (Al) and its alloys because only the acidic compositions are active for Al plating and stripping at the anode, according to the reversible redox reaction $[4(Al_2Cl_7)^- + 3e^- \leftrightarrow 7(AlCl_4)^- + Al]$.[102,103]

Linga et al.[104] investigated the electrochemistry of Ti^{4+} in $AlCl_3$-BupyCl (butyl pyridinium chloride) melts of basic composition. It was found that Ti^{4+} species is reduced to Ti^{3+} at −0.343 V vs an aluminum electrode, and the final reduction product in $AlCl_3$-BupyCl melt was Ti^{3+} species ($TiCl_6^{3-}$). Carlin et al.[105] reported the electrochemistry of $TiCl_4$ in $AlCl_3$-EmimCl (1-ethyl-3-methylimidazolium chloride) of acidic composition (molar ratio 1.5:1.0). In this strong Lewis acidic melt, Ti^{4+} species are reduced to Ti^{3+} species (β-$TiCl_3$) and Ti^{2+} via two one-electron steps. Takenaka et al.[106] studied the electroplating of Al-Ti alloy on Ni substrate from $TiCl_n$ (n = 2, 3, 4)-$AlCl_3$-BPC (n-butyl pyridinium chloride) melt at 27–177 °C. Smooth and dense deposits of Al and Ti (up to 27 at.%) were formed on the substrate. However, Al-Ti intermetallic compounds were not detected; even the electrodeposit consisted of more than 10 at.% Ti. Ali et al.[107] studied the electrochemistry of $TiCl_4$ in $AlCl_3$-BPC (n-butyl pyridinium chloride) melt, and it was found that the reduction of $TiCl_4$ proceeds in three consecutive steps [$Ti^{4+} \rightarrow Ti^{3+} \rightarrow Ti^{2+} \rightarrow Ti^0$]. In addition, they carried out electrodeposition of Al-Ti alloys on Pt cathode from $TiCl_4$-$AlCl_3$-BPC (n-butyl pyridinium chloride) melt (6.14:3.07:0.09 molar ratio) at 25 °C. They reported that it is challenging to electrodeposit pure Ti from this melt, but Al-Ti alloys containing up to 27 at.% Ti was obtained at the potential of −0.06 V (vs Al/Al^{3+}). The Al-Ti deposits layer was smooth and bright metallic appearance with a thickness of about 7 μm. The cathodic current efficiency of the electrodeposition was about 97%.

Tsuda et al.[108] conducted the electrodeposition of Al-Ti alloys on Cu rotating disk and wire electrode from acidic $AlCl_3$-EmimCl containing $TiCl_2$ at 80 °C. Al-Ti alloys containing up to 19 at.% Ti was electrodeposited at low current densities, and the increase of current density (2.5 to 20 mA cm^{-2}) resulted in the decrease of titanium content (19.1 to 12.4 atom %) in Al-Ti alloys. Besides, they reported that a small amount of purple precipitate identical to solid $TiCl_3$ was present in the melt (1.5:1.0 molar ratio) after the dissolution of $TiCl_2$. Still, the precipitate was not evident in the 2.0:1.0 molar ratio melt. The insoluble passivating $TiCl_3$ film acts as a block and prevents the oxidation of Ti^{2+} to Ti^{4+}. However, at high current density or positive potential, the passive layer breaks down, and Ti^0 could be oxidized directly to Ti^{4+}.

Mukhopadhyay et al.[109] reported the electrodeposition of Ti on an Au(111) substrate from 1-methyl-3-butyl-imidazolium bis (trifluoromethyl sulfone) imide ([BMIM] BTA) containing 0.24 M $TiCl_4$ at room temperature. According to results from cyclic voltammetry, Ti^{4+} was first reduced to Ti^{2+} at the potential of −0.39 V (vs Pt reference electrode). Then Ti^{2+} was reduced to metallic Ti at −1.45 V. At an applied potential of −1.1 V, and the Au substrate was covered with a thin layer of β-$TiCl_3$. However, a dense layer of three dimensional (3D) clusters of Ti with a thickness of 1–2 nm was obtained at the potential of −1.8 V.

Pradhan et al.[15] carried out the electrodeposition of Al-Ti alloys from $AlCl_3$-BmimCl-$TiCl_4$ (2:1:0.019 molar ratio) using a

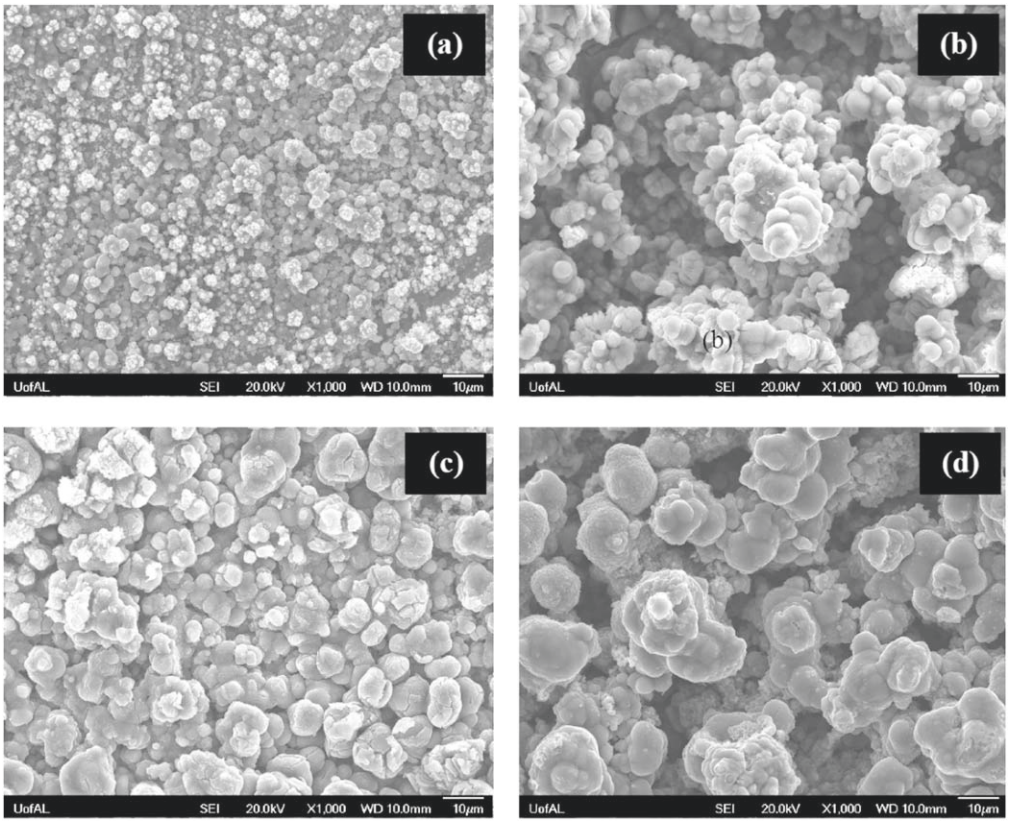

Figure 17. SEM micrographs of Ti-Al alloy electrodeposits from $AlCl_3$-BmimCl-$TiCl_4$ using different voltages (a) 1.5 V, (b) 2.0 V, (c) 2.5 V, and (d) 3.0 V at 100 °C.[15]

2-electrode system at different voltages (1.5–3.0 V) and temperatures (70 °C–125 °C). Ti foils were used as cathode and anode, and Ti wire was used as a reference electrode. The possible reactions were given by Eqs. 27–30. The Al-Ti alloys containing 14.95–26.57 at.% Ti were produced with current efficiencies of 25.07%–38.36% and energy consumptions of 16.63–31.98 kW·h kg^{-1}. As shown in Fig. 17, a more uniform and compact deposition with a particle size of 2–5 μm was found at lower applied cell voltage (1.5 V). To minimize the insoluble $TiCl_3$ passive layer formation, Pradhan et al.[110] produced Al-Ti alloys from $AlCl_3$-BmimCl (2:1 molar ratio) at similar experimental conditions. It was reported that better current efficiencies (78.57%–87.30%) and low energy consumptions (3.92–9.47 kW·h kg^{-1}) were achieved with $AlCl_3$-BmimCl.

$$\text{Cathode reactions: } [Ti(Al_2Cl_7^-)_4]^{2-} + 2e^- \rightarrow Ti(Cathode) + 4Al_2Cl_7^- \quad [27]$$

$$4Al_2Cl_7^- + 3e^- \rightarrow Al(Cathode) + 7AlCl_4^- \quad [28]$$

$$\text{Anode reactions: } Ti(anode) + 4Al_2Cl_7^- - 2e^- \rightarrow [Ti(Al_2Cl_7^-)_4]^{2-} \quad [29]$$

$$AlCl_3 + 7AlCl_4^- - 3e^- \rightarrow 4Al_2Cl_7^- + 1.5Cl_2 \quad [30]$$

Xu et al.[111] obtained Al-Ti alloy on mild steel substrate in $AlCl_3$-BmimCl (2:1 molar ratio) ionic liquids containing $TiCl_4$. The titanium content of the Al-Ti alloys, which were controlled by the applied current densities and $TiCl_4$ addition, ranged from 5.3 at.% to 11.4 at.%. Besides, they investigated the electrochemical behaviors of titanium in $AlCl_3$-BmimCl ionic liquids. The reduction of Ti^{4+} was a three-step process ($Ti^{4+} \rightarrow Ti^{3+} \rightarrow Ti^{2+} \rightarrow Ti^0$).[112] However, the electrodeposition of titanium is complicated by the precipitation of $TiCl_3$ and the oxidation of titanium to titanium ions at higher valence states such as Ti^{4+}, Ti^{3+}, and Ti^{2+} ions. Thus, it is challenging to deposit pure titanium in $AlCl_3$-BmimCl ionic liquids.

Pradhan and Reddy[113] demonstrated electrodeposition of Al-Ti alloys on the copper substrate at a constant potential (from 1.5 to 3 V) from $AlCl_3$-BmimCl-$TiCl_4$ (molar ratio of 2:1:0.019) ionic melt at low temperature (100 °C). Ti ions came from two sources, one from the addition of $TiCl_4$ and another from the dissolution of Ti ions from Ti anode. The titanium content was maximum at 1.5 V. It decreased from 25.47 at.% to 10.57 at.% as applied potential increased to 3 V. Al-Ti deposition resulted in granular morphology with finer particles at 1.5 V and consisted of Al and disordered Al_3Ti phases.

Bogala et al.[114] conducted the constant-current electrodeposition of Al-Ti alloys from $AlCl_3$-BmimCl (2:1 molar ratio) at 100 °C and high cathode current densities (135–891 A m^{-2}). Figure 18 shows the image of Ti electrodes before and after the electrodeposition experiment at 100 °C at 891 A m^{-2} for 4 h. It was evident that the immersed portion of Ti anode was dissolved entirely in the melt according to reaction (29). The electrodeposits containing 14.56 to 20.75 at.% Ti were obtained with current efficiencies of 60.96%–81.35% and energy consumptions of 6.71–12.08 kW·h kg^{-1}.

Pradhan and Reddy[115] have performed electrodeposition of titanium using BmimCl ionic liquid at higher cathode current densities at 100 °C to improve the deposition rates. A mixed scrap anode was dissolved in the electrolyte served as the source of titanium. Figure 19 shows the variation of cathode voltage with time at different applied current densities. The potential steps in each of the curves signify the plot at a different level of reactions. At lower potential (<1.0 V), $TiCl_4$, which is formed during the anodic dissolution of titanium, gets reduced to $TiCl_3$ and Ti, signifying a violet-colored passivating layer of $TiCl_3$ on the cathode. As the

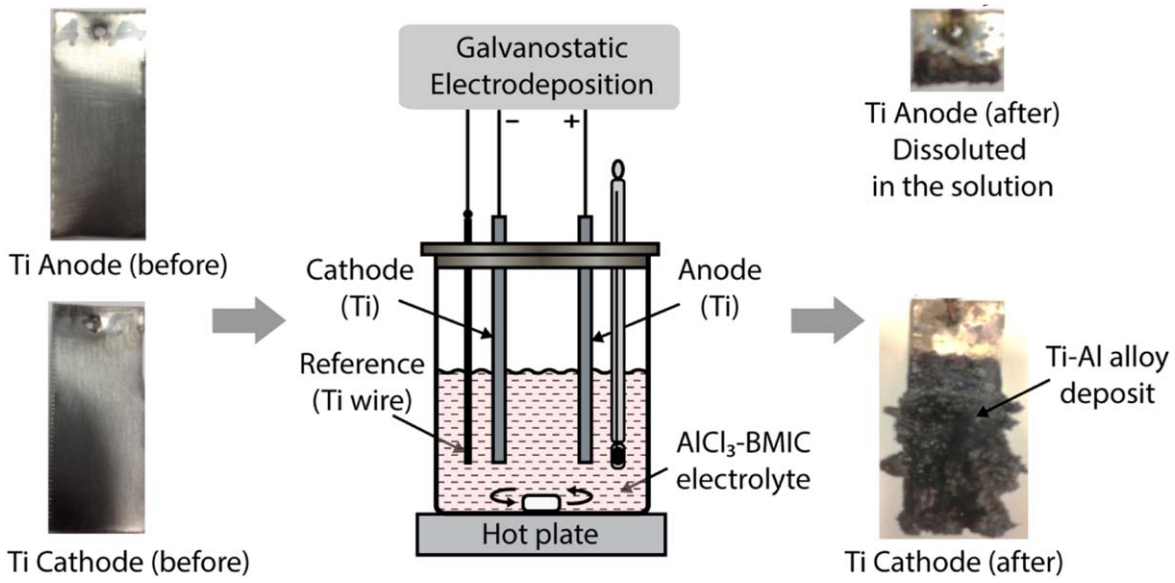

Figure 18. Images of Ti electrodes before and after the galvanostatic electrodeposition of Ti-Al alloy from $AlCl_3$-BmimCl (2:1 molar ratio) at 100 °C at 891 A m^{-2}.[114]

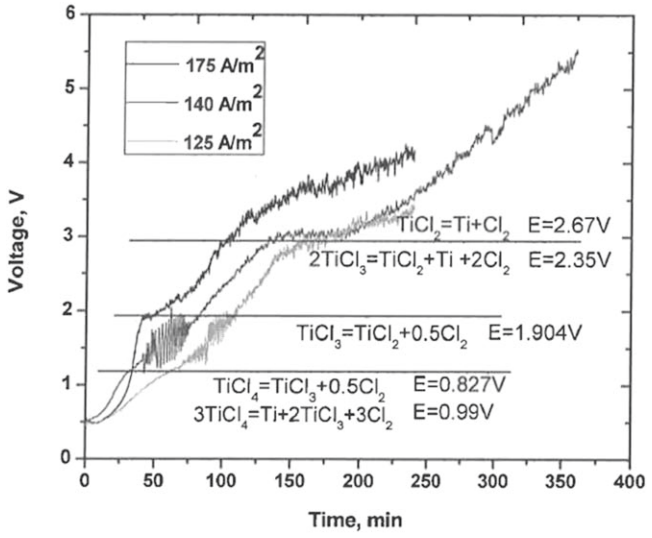

Figure 19. Variation of cathodic voltage with time for different cathode current densities (125, 140, and 175 A m^{-2}) at 100 ± 3 °C.[115]

potential exceeds 2.5 V, $TiCl_3$ passivating layers break down, and Ti is deposited on the cathode. This is a major advantage of the process. At higher cathode current densities or cathode potentials, $TiCl_3$ passivating layers break down, and high purity Ti can be deposited on the cathode. At lower current densities, larger particles were deposited on the cathode (40–50 um using 125 A m^{-2}). But as the current density increases, the particle size decreases (5–10 um using 170 A m^{-2}). This produces a larger number of nucleation sites resulting in smaller size particles. These results show that a constant current density method to produce Ti has a significant improvement in the deposition rates. The best process conditions to produce Ti are at cathode current density of >170 A m^{-2}, which can give higher deposition rates with higher current efficiency (>80%). Such optimum conditions can produce pure Ti deposits with a finer particle size of Ti (5–10 um).

Recently, the electrosynthesis of smooth Ti-Al alloy on copper substrates has been demonstrated by our group using $AlCl_3$–BmimCl ionic liquid at relatively low temperatures. A potentiostatic electrodeposition is employed using a 3-electrode configuration.[116] The cyclic voltammetry studies are performed on platinum to understand Ti and Al ions' deposition conditions with titanium wire as sacrificial donor source of Ti ions during the electrodeposition from $AlCl_3$–BmimCl ionic liquid with a molar ratio of 2:1 at 100 °C. Ti-Al alloys produced at a relatively lower applied voltage (−1.0, −1.3 V) are dark, uniform, dendrite-free, and compact in nature (Fig. 20a). The amount of Ti in the Ti-Al is 3% for 1 h deposition at −1.3 V vs Ti, which could be improved further by controlling Ti species' concentration in the ionic liquid electrolyte (Fig. 20b).

Several different titanium-alloys Ti-W,[117,118] Ti-Fe,[119,120] Ti-Ni,[121] Ti-Ni-Hf,[122] Ti-Ni-Nb,[123] Ti-Mo,[124] Ti-Si,[125] Ti-Al,[126] and Ti-Nb-Ta-Zr[127] have been produced by either the FFC process or the OS processes.

The efforts are also being made to obtain Ti by electrorefining process at high temperature (750 °C) from potassium-free $BaTiF_6$ as a solvent in fluoride molten salt. A novel approach of Ti ingot preparation is described, where electrorefining of Ti from Cu-Ti alloy is one of the technological steps. The Ti electrorefining process was investigated by chronopotentiometry method using the CuTi rod as an anode (counter electrode). The electrolysis of Ti was performed at various conditions (current density, temperature) to study the morphology of deposited Ti. Titanium's crystal size was up to 200 μm in most cases, which allowed successful separation of the deposit from the salt and then to obtain theTi ingot by arc melting process.[128]

Thermal Plasma and Plasma Arc Melter Method

TiB_2 was prepared using the thermal plasma processing technique.[129] In this technique, the production of TiB_2 by thermal plasma was performed using TiO_2 and B_2O_3 as solid feed in the presence of CH_4 as reducing gas. The molar ratio of the reducing gas in the TiO_2-B_2O_3-CH_4 system was varied. The maximum yield of TiB_2 (40 mol%) was obtained with a feed molar ratio of TiO_2:B_2O_3:CH_4 = 1:1:5. Alternatively, Ramachandran and Reddy[130] have reported a facile self-propagating high-temperature synthesis (SHS) method to synthesize titanium diboride (TiB_2) and Ti-Al-B composites. Such a one-stem process involves the single phase-pure formation of TiB_2 using pellets of titanium and boron powders in a plasma arc Melter. TiB_2 formed is porous with particle sizes in the range of 10–20 μm. High temperatures resulting from exothermic reaction lead to consolidation of TiB_2 particles and grain growth. A similar one-step synthesis procedure can be used to obtain TiAl-TiB_2 composites.

Table V. Summary of emerging Ti production technologies.

Processes	Features	Advantages	Disadvantages	References
The Hunter and Kroll process	The reduction of $TiCl_4$ by Liquid Na or Mg	Product with less oxygen content and metallic impurities	Low productivity; The high cost of reductant; High energy consumption	Turner et al. (2001)[19]
Electrolysis in LiF-NaF-KF	The electrolytic reduction of K_2TiF_6 at 750 °C in LiF-NaF-KF	High current efficiency (80%–85%); Continuous operation	Formation of insoluble Ti^{3+} layer; redox cycling; Dendritic titanium coatings	Robin et al. (2005)[30]
Electrolysis in cryolite-base melt	The electrolysis of TiO_2 at 960 °C in Na_3AlF_6-base melts, Liquid Al as a cathode.	Continuous operation	Use of high temperature; Difficult to produce pure titanium	Yan et al. (2016)[42]
USTB process	Electrolysis at 800 °C and −0.45 V vs Ag/AgCl in NaCl-KCl melt; TiC_xO_{1-x} solid solutions used as the anode	Product with low oxygen content (0.3 mass %); Semi-continuous operation	Dendritic titanium deposition; Difficult to fabricate the composite anode; Low current efficiency (15%–50%)	Zhu et al. (2006)[58]
FFC process	Electrolysis at 900 °C and 2.8–3.2 V in $CaCl_2$ melts; Preformed TiO_2 pellet as the cathode	Product with low oxygen content (0.3 mass% oxygen); Semi-continuous operation	Low current efficiency (20%–40%); slow oxygen diffusion; difficult separation of metal/salt	Wang et al. (2006)[64]
OS process	Calciothermic reduction of TiO_2 Powder at 900 °C in $CaCl_2$-CaO melts; Electrolytic reduction of CaO to Ca at 2.6–2.9 V	Product with low oxygen content (0.2 mass% oxygen); TiO_2 Powder as feed; semi-continuous operation	Low current efficiency (8.8%–25.5%); sensitive to carbon and iron contamination; difficult separation of metal/salt	Suzuki et al. (2003)[73]
PRP process	Reduction of feed preform (a mixture of TiO_2 + $CaCl_2$ or CaO) by Ca vapor at 800 °C–1000 °C	High purity (99 mass%) and homogeneous fine titanium powder	The high cost of reductant (Ca)	Okabe et al. (2004)[80]
EMR process	TiO_2 is reduced by electrons discharged from the reductant (Ca-Ni alloy) at 900 °C in $CaCl_2$ molten salt	Product with High purity (99.5 mass %); Resistant to carbon and contamination; Continuous operation	Complicated process and cell structure; difficult separation of metal and salt	Park et al. (2005)[82]
Electrolysis in ionic liquids	Electrolytic reduction of $TiCl_4$ in ionic liquid ($AlCl_3$-BmimCl) at 70°C–125°C; Products were Al-Ti alloys	Low temperature; high current efficiency (78.57%–87.30%); Low energy consumption	Difficult to produce pure titanium; Expensive ionic liquid	Pradhan et al. (2009)[15]
Electrorefining from molten salt	Electrorefining of Titanium from CuTi anode in K-Free Molten Salt; High temperature (750 °C);	Novel K-free $BaTiF_6$ as a solvent; CuTi rod as an anode, 200 μm size Ti crystal size, Easy to separate	High temperature, High energy consumption	Ri et al. (2019)[128]
Armstrong process	Reduction of $TiCl_4$ and other metal halides using Na to obtain pure Ti; The powder particles produced posses' unique properties and low bulk density.	Produce commercially pure Ti (CP-Ti) powder, powder's morphology provides excellent compressibility and compactness.	Irregular morphology due to granular agglomerates of smaller particles.	Ovchinnikov et al. (2018)[85]
HDH process	HDH process produces Ti powder using Ti sponge, titanium, mill products, or titanium scrap as the raw material.	Hydrogenation conditions of Ti: 1 atm pressure and 800 °C temperature. Very high purity of Ti powder. Relatively inexpensive process.	High temperature; Irregular and angular powder morphology; Not suitable for making virgin alloyed powders or alloy composition modifications from raw scrap material	Fang et al. (2018)[86]
MAFBR Plasma-arc process	MAFBR process produces Ti powder using Ti ores ($TiCl_4$) as the raw material in less steps and less energy-intense way	10 s of μm size Ti particles, Easy to shape the powder, uses atomic hydrogen as reducing agent, direct production of alloys possible.	Involves disproponation reaction of arc plasma with $TiCl_4$ forming solid $TiCl_2$ that is hard to reduce.	Sanjurjo et al. (2013)[88]
Aluminothermic reduction process	Two-stage aluminothermic reduction of Ti-containing cryolite and aluminium	Spherical or near-spherical Ti-6Al-4V alloy with uniform distribution of Al and V.	High temperature (1050 °C) requirement	Wang et al. (2020)[90]
			High temperature (1050 °C) requirement	

Table V. (Continued).

Processes	Features	Advantages	Disadvantages	References
Low-temperature reduction using MgH_2	$TiCl_4$ reduction to TiH_2 using MgH_2 under H_2 and then to Ti powder by dehydrogenation at 400 °C–500 °C.	Low-cost Ti powder, Low oxygen content Ti, Low energy consumption.		Ardani et al. (2020)[95]
HAMR process	Two-step process: Mg reduction in H_2 followed by a deoxygenation step in H_2 at ∼800 °C.	Low oxygen content in Ti (<0.15wt. %); Can produce Ti in the form of TiH_2	High temperature (700 °C–800 °C), High energy consumption	Fang et al. (2016)[96]

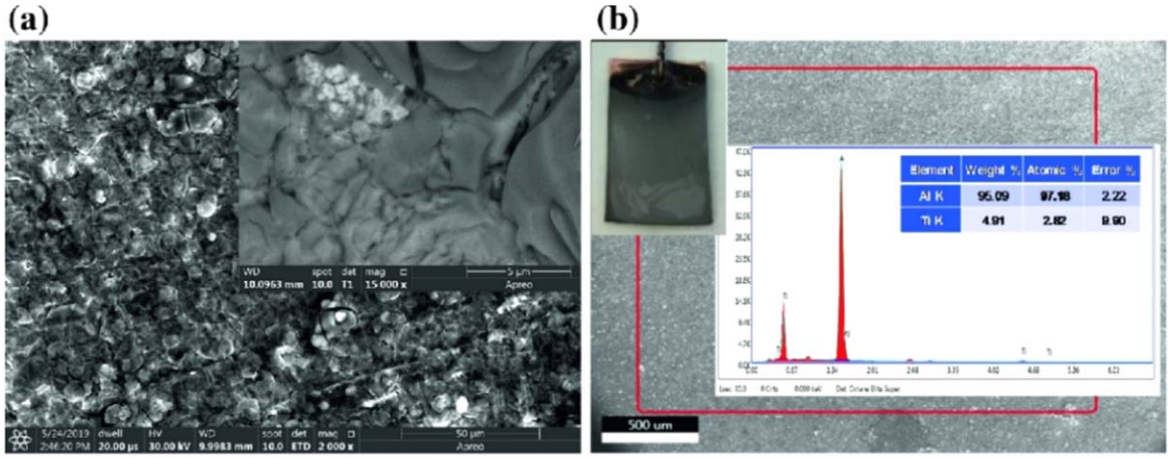

Figure 20. (a) SEM image (2000X) of Ti-Al alloy deposited on Cu substrate at −1.3 V vs Ti for 1 h and (b) corresponding EDS spectrum (inset showing a photo of the electrode).[116]

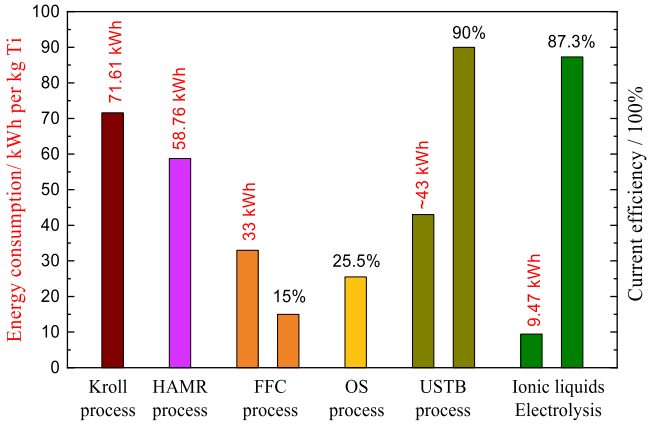

Figure 21. Energy consumption and the current efficiency of typical emerging electrolytic processes for titanium production.[16,17,61,62,110,131]

Emerging Ti Production Technologies

Table V summarizes the various titanium production technologies, including the widely utilized Kroll process. A brief description of the process, the main features of the technology, advantages, and disadvantages are tabulated. The advantages include product output with less oxygen content and impurities, continuous operation, homogeneity, low-cost, energy-efficient, high current efficiency, and ease of processes. The disadvantages include low productivity, high cost, high energy consumption, complicated and multi-step processing, toxicity, impurities, high-temperature requirement.

As shown in Fig. 21, the current efficiency (87.3%) and energy consumption (9.47 kWh kg^{-1} Ti)[110] for titanium reduction using $AlCl_3$-BmimCl ionic liquids are much better than those involved in the Kroll process[17] and other typical innovative electrolytic extraction techniques. FFC process consumes relatively less energy. However, it has poor current efficiency. OS process also has low current efficiency. Although the USTB process has shown promising current efficiency of >90%,[16] its energy consumption is 40% of the Kroll process, which is still a higher value.[131] Despite the emergence of numerous other electrolytic methods, none of them reached industrialization. So far, USTB and ionic liquid electrolysis look promising in terms of current efficiency. The major hurdles have been the low current efficiency due to the formation of multi-valent titanium ions, obstacles of separating the titanium deposit and the electrolytic solutions, low productivity due to a slower reaction rate compared to the one in metallothermic reduction, and low space utilization efficiency in the electrolytic cell.[10]

To make titanium a general-purpose metal, the Ti reduction process has to be high speed, energy-efficient, low-cost with low environmental impact. Considering the higher current efficiency and little energy consumption, Ti-production by electrolysis from ionic liquids offer a low-cost and high efficiency that has the potential for industrial scale-up. Additionally, there would be a rise in the supply of low-grade titanium in case the demand for titanium metal increases dramatically in the future. Hence, there is scope for the development of efficient and contaminant-free (for example, oxygen and iron) processes for the efficient utilization of titanium. Thus, the advances in these technologies is crucial for the break-through innovations in the titanium industry.

Conclusions

A widespread and cost-affordable commercial production and use of titanium is hampered by the disadvantages of improved Kroll process including high cost and high energy consumption. Over the years, many innovative electrolytic extraction techniques have been developed and aimed to replace the Kroll process. Among the new methods, electrochemical reduction of K_2TiF_6 from LiF-NaF-KF melts is advantageous in terms of high current efficiency (80%–85%) and continuous operation. However, disadvantages such as redox cycling and dendritic titanium coatings limits its usage. It is impossible to produce pure titanium from electrolysis of TiO_2 from Na_3AlF_6-base melts at high temperature (~1000 °C), which aims to achieve similar success of the Hall–Héroult process. The USTB process can produce titanium with low oxygen content (0.3 mass %), but it suffers from a dendritic titanium deposition. The requirement for the fabrication of the composite TiC_xO_{1-x} anode is also a drawback. The EMR process has the advantages of the product with high purity (99.5 mass %) and the potential for continuous operation. However, the cell structure is complicated, and further study is required to identify the mechanism and optimum EMR process parameters. Besides, the PRP process is also not suitable for commercial applications because of the expensive reductant (Ca). A two-step HAMR process is advantages in terms of producing Ti with low-oxygen content (< 0.15 wt.%). Moreover, it obtains titanium in the form of TiH_2, which is less prone to being oxidized. However, this process is not energy-efficient. Both the FFC and OS processes have the potential to produce titanium powder semi-continuously with low oxygen content (0.3 mass% oxygen). However, long-term studies are required to improve the current efficiency of both the FFC and OS processes. Apart from the FFC and OS processes, it should be noted that the electrolytic reduction of $TiCl_4$ from ionic liquids such as $AlCl_3$-BmimCl is an alternatively promising method to produce cost-effective titanium. The temperature (75 °C–125 °C) required is much lower than other existing titanium extraction

techniques. Innovation and cost-reduction methods are continuously developed to produce the low-cost titanium. The new advances in production technologies would allow the titanium industries to enter a new era of expansion.

Acknowledgments

The authors acknowledge the financial support from the National Science Foundation (NSF) award number 1762522 and ACIPCO for this research project. The authors also thank the Department of Metallurgical and Materials Engineering, the University of Alabama, for providing the experimental and analytical facilities.

ORCID

Ramana G. Reddy https://orcid.org/0000-0002-4214-637X
Pravin S. Shinde https://orcid.org/0000-0002-1715-6867

References

1. E. H. Kraft, *Report by EHK Technologies, Vancouver, WA, Canada* (2004), https://www.yumpu.com/en/document/read/8707577/summary-of-emerging-titanium-cost-reduction-technologies.
2. M. Peters, J. Kumpfert, C. H. Ward, and C. Leyens, *Adv. Eng. Mater.*, **5**, 419 (2003).
3. I. Inagaki, T. Takechi, Y. Shirai, and N. Ariyasu, *Nippon steel & sumitomo metal technical report*, 22, 106 (2014), https://www.nipponsteel.com/en/tech/report/nssmc/pdf/106-05.pdf.
4. C. Elias, J. Lima, R. Valiev, and M. Meyers, *JOM*, **60**, 46 (2008).
5. M. Niinomi, M. Nakai, J. Hieda, K. Cho, T. Akahori, T. Hattori, and M. Ikeda, *Key Eng. Mater.*, **551**, 133 (2013).
6. F. H. S. Froes, M. N. Gungor, and M. A. Imam, *JOM*, **59**, 28 (2007).
7. D. Bernhardt and I. I. J. F. Reilly, *U.S. Geological Survey* (Mineral Commodity Summaries, Reston, VA) p. 20 (2020).
8. T. Takenaka, H. Matsuo, and M. Kawakami, *ISIJ Int.*, **51**, 1762 (2011).
9. X.-M. Nie, L.-Y. Dong, C.-G. Bai, D.-F. Chen, and G.-B. Qiu, *Transactions of Nonferrous Metals Society of China*, **16**, s723 (2006).
10. O. Takeda, T. Ouchi, and T. H. Okabe, *Metallurgical and Materials Transactions B*, **51**, 1315 (2020).
11. F. Froes, *Titanium: Physical Metallurgy, Processing, and Applications* (ASM international, Materials Park, Ohio) (2015), https://app.knovel.com/hotlink/toc/id:kpTPMPA00D/titanium-physical-metallurgy/titanium-physical-metallurgy.
12. G. Z. Chen, D. J. Fray, and T. W. Farthing, *Nature*, **407**, 361 (2000).
13. K. Ono and R. O. Suzuki, *JOM*, **54**, 59 (2002).
14. S. Jiao and H. Zhu, *J. Alloys Compd.*, **438**, 243 (2007).
15. D. Pradhan and R. G. Reddy, *Electrochim. Acta*, **54**, 1874 (2009).
16. H. Zhu, S. Jiao, J. Xiao, and J. Zhu, *Extractive Metallurgy of Titanium* (Elsevier, Amsterdam) p. 315 (2020).
17. Y. Xia, H. D. Lefler, Z. Z. Fang, Y. Zhang, and P. Sun, *Extractive Metallurgy of Titanium* (Elsevier, Amsterdam) p. 389 (2020).
18. M. A. Hunter, *J. Am. Chem. Soc.*, **32**, 330 (1910).
19. P. C. Turner, A. D. Hartman, J. S. Hansen, and S. J. Gerdemann, *Low Cost Titanium-Myth or Reality* (Albany Research Center (ARC), Albany, OR) (2001), https://digital.library.unt.edu/ark:/67531/metadc884250/.
20. D. Demeter, Titanium industries - one metal, a thousand possibilities (2009), http://www.titaniumexposed.com/titanium-industries.html.
21. D. Hu and G. Z. Chen, "Advanced Extractive Electrometallurgy." *Springer Handbook of Electrochemical Energy* (Springer, Berlin) p. 801 (2017).
22. A. R. Stetson, *Electrolytic production of titanium plate*, U.S. Patent No. 3,024,174 (1962).
23. F. Clayton, G. Mamantov, and D. Manning, *J. Electrochem. Soc.*, **120**, 1193 (1973).
24. J. De Lepinay, J. Bouteillon, S. Traore, D. Renaud, and M. Barbier, *J. Appl. Electrochem.*, **17**, 294 (1987).
25. A. Robin, J. D. Lepinay, and M. Barbier, *J. Appl. Electrochem.*, **20**, 289 (1990).
26. A. Robin and J. D. Lepinay, *Electrochim. Acta*, **36**, 1009 (1991).
27. A. Robin, J. D. Lepinay, and M. Barbier, *J. Electroanal. Chem. Interf. Electrochem.*, **230**, 125 (1987).
28. A. Robin, *Mater. Lett.*, **34**, 196 (1998).
29. A. Robin and R. Ribeiro, *J. Appl. Electrochem.*, **30**, 239 (2000).
30. A. Robin, *Mater. Chem. Phys.*, **89**, 438 (2005).
31. J. Li and B. Li, *Chin. J. Nonferr. Met.*, **16**, 144 (2006), http://www.airitilibrary.com/Publication/alDetailedMesh?DocID=10040609-200606-201204100014-201204100014-144-149.
32. J. Li and B. Li, *Rare Metal Mat. Eng.*, **36**, 15 (2007).
33. Å. Sterten, P. Solli, and E. Skybakmoen, *J. Appl. Electrochem.*, **28**, 781 (1998).
34. Z.-X. Qiu, M.-J. Zhang, Y.-X. Yue, and Z. Che, *Aluminium*, **64**, 606 (1988).
35. Z. Liu, M. Song, and T. Song, *China Foundry*, **2**, 7 (2005), https://www.ingentaconnect.com/content/doaj/16726421/2005/00000002/00000001/art00002.
36. X.-G. Yu and Z.-X. Qiu, *Journal of Northeastern University (Natural Science)*, **25**, 442 (2004), http://xuebao.neu.edu.cn/natural/EN/volumn/volumn_1296.shtml.
37. Y. Hayakawa and H. Kido, *Electrochem.*, **20**, 263 (1952).
38. A. Beljaew, L. Firsanowa, and M. B. Rapoport, *Metallurgie des Aluminiums* (VEB Verlag Technik, Berlin) v.1 : Die Elektrolyse von Kryolith-Tonerde-Schmelzen, 74 (1956), https://books.google.com/books?id=OvgAzgEACAAJ.
39. T. P. Madhavan, K. Matiašovský, and V. Daněk, *Chem. Pap.*, **25**, 253 (1971), https://www.chempap.org/?id=7&paper=5881.
40. A. Sterten and O. Skar, *Aluminium*, **64**, 1051 (1988).
41. T. E. Jentoftsen, O.-A. Lorentsen, E. W. Dewing, G. M. Haarberg, and J. Thonstad, *Metall. Mater. Trans. B*, **33**, 909 (2002).
42. B. C. K. Yan, *Electrolysis of Titanium Oxide to Titanium in Molten Cryolite Salt*, Thesis, University of Toronto, Canada (2016), http://hdl.handle.net/1807/72839.
43. S. Devyatkin, G. Kaptay, J. Poignet, and J. Bouteillon, *High Temp. Mater. Processes (New York)*, **2**, 497 (1998).
44. Z. Qin, W. Z. Li, L. M. Lv, and S. Yang, *Light Metals*, **7**, 47 (2006), http://en.cnki.com.cn/Article_en/CJFDTOTAL-QJSS200607012.htm.
45. H.-B. Sun, Z.-G. Zhong, X.-R. Zuo, and X.-H. Hu, *J. Electrochem.*, **14**, 104 (2008), http://electrochem.xmu.edu.cn/CN/Y2008/V14/I1/104.
46. M. Gibilaro, J. Pivato, L. Cassayre, L. Massot, P. Chamelot, and P. Taxil, *Electrochim. Acta*, **56**, 5410 (2011).
47. E. Chassaing, F. Basile, and G. Lorthioir, *J. Appl. Electrochem.*, **11**, 187 (1981).
48. D. Ferry and G. Picard, *J. Appl. Electrochem.*, **20**, 125 (1990).
49. C. Guang-Sen, M. Okido, and T. Oki, *Electrochim. Acta*, **32**, 1637 (1987).
50. F. Lantelme, K. Kuroda, and A. Barhoun, *Electrochim. Acta*, **44**, 421 (1998).
51. F. Lantelme and A. Salmi, *J. Electrochem. Soc.*, **142**, 3451 (1995).
52. X. Ning, H. Åsheim, H. Ren, S. Jiao, and H. Zhu, *Metallurgical and Materials Transactions B*, **42**, 1181 (2011).
53. M. H. Kang, J. Song, H. Zhu, and S. Jiao, *Metallurgical and Materials Transactions B*, **46**, 162 (2015).
54. Y. Song, S. Jiao, L. Hu, and Z. Guo, *Metallurgical and Materials Transactions B*, **47**, 804 (2016).
55. D. Ferry, G. Picard, and B. Tremillon, *J. Electrochem. Soc.*, **135**, 1443 (1988).
56. C. Guang-Sen, M. Okido, and T. Oki, *J. Appl. Electrochem.*, **18**, 80 (1988).
57. J. H. Von Barner, P. Noye, A. Barhoun, and F. Lantelme, *J. Electrochem. Soc.*, **152**, C20 (2004).
58. S. Jiao and H. Zhu, *J. Mater. Res.*, **21**, 2172 (2006).
59. S. Jiao, X. Ning, K. Huang, and H. Zhu, *Pure Appl. Chem.*, **82**, 1691 (2010).
60. C. R. Nagesh and C. S. Ramachandran, *Transactions of Nonferrous Metals Society of China*, **17**, 429 (2007).
61. D. Hu, A. Dolganov, M. Ma, B. Bhattacharya, M. T. Bishop, and G. Z. Chen, *JOM*, **70**, 129 (2018).
62. W. Li, X. Jin, F. Huang, and G. Z. Chen, *Angew. Chem.*, **122**, 3271 (2010).
63. G. Z. Chen and D. J. Fray, *J. Electrochem. Soc.*, **149**, E455 (2002).
64. S. Wang and Y. Li, *J. Electroanal. Chem.*, **571**, 37 (2004).
65. K. Dring, R. Dashwood, and D. Inman, *J. Electrochem. Soc.*, **152**, E104 (2005).
66. B. Wang, K.-R. Liu, and J.-S. Chen, *Transactions of Nonferrous Metals Society of China*, **21**, 2327 (2011).
67. C. Schwandt and D. J. Fray, *Electrochim. Acta*, **51**, 66 (2005).
68. D. T. L. Alexander, C. Schwandt, and D. J. Fray, *Electrochim. Acta*, **56**, 3286 (2011).
69. M. Ma, D. Wang, W. Wang, X. Hu, X. Jin, and G. Z. Chen, *J. Alloys Compd.*, **420**, 37 (2006).
70. L. I. U. Meifeng, L. U. Shigang, S. Kan, and L. I. Guoxun, *Rare Met.*, **26**, 547 (2007).
71. D. S. Maha Vishnu, N. Sanil, L. Shakila, R. Sudha, K. S. Mohandas, and K. Nagarajan, *Electrochim. Acta*, **159**, 124 (2015).
72. R. O. Suzuki and S. Inoue, *Metallurgical and Materials Transactions B*, **34**, 277 (2003).
73. R. O. Suzuki, K. Ono, and K. Teranuma, *Metallurgical and Materials Transactions B*, **34**, 287 (2003).
74. R. O. Suzuki and S. Fukui, *Mater. Trans.*, **45**, 1665 (2004).
75. R. O. Suzuki, *J. Phys. Chem. Solids*, **66**, 461 (2005).
76. K. Kobayashi, Y. Oka, and R. O. Suzuki, *Mater. Trans.*, **50**, 2704 (2009).
77. M. A. Imam, F. Froes, and R. G. Reddy, *Key Eng. Mater.*, **551**, 3 (2013).
78. D. Mangabhai, K. Araci, M. K. Akhtar, N. A. Stone, and D. Cantin, *Key Eng. Mater.*, **551**, 57 (2013).
79. M. R. Bogala and R. G. Reddy, *J. Manuf. Sci. Prod.*, **16**, 1 (2016).
80. T. H. Okabe, T. Oda, and Y. Mitsuda, *J. Alloys Compd.*, **364**, 156 (2004).
81. J. G. Jia, B. Q. Xu, B. Yang, D. S. Wang, H. Xiong, and D. C. Liu, *Key Eng. Mater.*, **551**, 25 (2013).
82. I. Park, T. Abiko, and T. H. Okabe, *J. Phys. Chem. Solids*, **66**, 410 (2005).
83. T. H. Okabe and Y. Waseda, *JOM*, **49**, 28 (1997).
84. D. S. Van Vuuren, S. J. Oosthuizen, and J. J. Swanepoel, *Key Eng. Mater.*, **551**, 16 (2013).
85. A. Ovchinnikov, Y. Smolyak, A. Dzhugan, E. Yunusov, T. Ianko, and S. Panov, Technology of new Generation Titanium Alloys Powder for Additive Technology (2018), https://www.ariel.ac.il/sites/conf/mmt/mmt-2016/Service%20files/papers/102-109.pdf.
86. Z. Z. Fang, J. D. Paramore, P. Sun, K. R. Chandran, Y. Zhang, Y. Xia, F. Cao, M. Koopman, and M. Free, *Int. Mater. Rev.*, **63**, 407 (2018).
87. F. Yang, D. L. Zhang, B. Gabittas, and H. Y. Lu, *Key Eng. Mater.*, **551**, 67 (2013).
88. A. Sanjurjo, K. Matsumoto, C. Colominas, G. Krishnan, P. Jayaweera, and K.-H. Lau, *Multiarc discharge moving bed reactor system*, US Patent No. US8465809B2 (2013), https://patents.google.com/patent/WO2007130613A3/en.
89. C. Doblin, D. Freeman, and M. Richards, *Key Eng. Mater.*, **551**, 37 (2013).
90. T. Wang and Y. Wang, *TMS 2020 149th Annual Meeting & Exhibition Supplemental Proceedings* (Springer, Cham.) p. 1681 (2020).

91. J. Withers, V. Shapovalov, R. Storm, and R. Loutfy, *Key Eng. Mater.*, **551**, 32 (2013).
92. J. Withers, V. Shapovalov, R. Storm, and R. Loutfy, *Key Eng. Mater.*, **551**, 11 (2013).
93. D. Zhang and S. R. Raynova, *Method for producing metal alloy and intermetallic products*, US Patent No. US0311123A1 (2009), https://www.freepatentsonline.com/WO2007139403.html.
94. K. Sichone, D. L. Zhang, and S. Raynova, *Key Eng. Mater.*, 44 (2013).
95. M. R. Ardani, S. A. R. S. A. Hamid, H. L. Lee, A. R. Mohamed, and I. Ibrahim, *149th Annual Meeting & Exhibition Supplemental Proceedings, The Minerals, Metals and Materials Society (eds) TMS 2020*, San Diego, CA (Springer, Cham.) p. 1669 (2020).
96. Z. Z. Fang, Y. Zhang, Y. Xia, and P. Sun, *Methods of producing a titanium product*, US Patent No. US10689730B2 (2016), https://patents.google.com/patent/US10689730B2/en.
97. Y. Zhang, Z. Z. Fang, Y. Xia, Z. Huang, H. Lefler, T. Zhang, P. Sun, M. L. Free, and J. Guo, *Chem. Eng. J.*, **286**, 517 (2016).
98. Y. Zhang, Z. Z. Fang, P. Sun, T. Zhang, Y. Xia, C. Zhou, and Z. Huang, *J. Am. Chem. Soc.*, **138**, 6916 (2016).
99. Z. J. Karpinski and R. A. Osteryoung, *Inorg. Chem.*, **23**, 1491 (1984).
100. M. Li, B. Gao, C. Liu, W. Chen, Z. Wang, Z. Shi, and X. Hu, *J. Solid State Electrochem.*, **21**, 469 (2017).
101. G. Zhu et al., *RSC Adv.*, **9**, 11322 (2019).
102. T. Jiang, M. J. Chollier Brym, G. Dubé, A. Lasia, and G. M. Brisard, *Surf. Coat. Technol.*, **201**, 1 (2006).
103. J. S. Wilkes, J. A. Levisky, R. A. Wilson, and C. L. Hussey, *Inorg. Chem.*, **21**, 1263 (1982).
104. Z. Stojek, H. Linga, and R. Osteryoung, *J. Electroanal. Chem. Interfacial Electrochem.*, **119**, 365 (1981).
105. R. T. Carlin, R. A. Osteryoung, J. S. Wilkes, and J. Rovang, *Inorg. Chem.*, **29**, 3003 (1990).
106. T. Takenaka and M. Kawakami, *Int. J. Mater. Prod. Technol.*, **500** (2001).
107. M. Ali, A. Nishikata, and T. Tsuru, *Indian J. Chem. Technol.*, **10**, 14 (2003), http://hdl.handle.net/123456789/22693.
108. T. Tsuda, C. L. Hussey, G. R. Stafford, and J. E. Bonevich, *J. Electrochem. Soc.*, **150**, C234 (2003).
109. I. Mukhopadhyay, C. L. Aravinda, D. Borissov, and W. Freyland, *Electrochim. Acta*, **50**, 1275 (2005).
110. D. Pradhan, R. Reddy, and A. Lahiri, *Metall. Mater. Trans. B*, **40**, 114 (2009).
111. C. Xu, Y. Hua, Q. Zhang, J. Li, Z. Lei, and D. Lu, *J. Solid State Electrochem.*, **21**, 1349 (2017).
112. C. Xu, Y. Liu, Y. Hua, J. Li, and Q. Zhang, *Mater. Trans.*, **58**, 377 (2017).
113. D. Pradhan and R. Reddy, "Production of Al-Ti alloys using ionic liquid electrolytes at low temperatures." *Innovation in titanium technology: Novel materials and processes I* (TMS, The Minerals, Metals and Materials Society, Orlando, FL) p. 79 (2007).
114. M. R. Bogala, *Electrodeposition of Titanium Aluminides from Aluminum Chloride: 1-butyl-3-Methyl Imidazolium Chloride Ionic Liquid*, Thesis, University of Alabama, AL, USA (2015), https://ir.ua.edu/handle/123456789/2312.
115. D. Pradhan and R. G. Reddy, "Electrodeposition of titanium using BmimCl ionic liquid at higher cathode current densities." *Unpublished work* (2021).
116. P. S. Shinde, Y. Peng, and R. G. Reddy, *149th Annual Meeting and Exhibition Supplemental Proceedings, The Minerals, Metals and Materials Society (eds) TMS 2020*, San Diego, CA (Springer, Cham.) p. 1659 (2020).
117. K. Dring, R. Bhagat, M. Jackson, R. Dashwood, and D. Inman, *J. Alloys Compd.*, **419**, 103 (2006).
118. R. Bhagat, M. Jackson, D. Inman, and R. Dashwood, *J. Electrochem. Soc.*, **156**, E1 (2008).
119. M. Panigrahi, E. Shibata, A. Iizuka, and T. Nakamura, *Electrochim. Acta*, **93**, 143 (2013).
120. M. Panigrahi, A. Iizuka, E. Shibata, and T. Nakamura, *J. Alloys Compd.*, **550**, 545 (2013).
121. B. Jackson, M. Jackson, D. Dye, D. Inman, and R. Dashwood, *J. Electrochem. Soc.*, **155**, E171 (2008).
122. B. Wang, R. Bhagat, X. Lan, and R. Dashwood, *J. Electrochem. Soc.*, **158**, D595 (2011).
123. R. Enmei, T. Kikuchi, and R. O. Suzuki, *Electrochim. Acta*, **100**, 257 (2013).
124. R. Bhagat, M. Jackson, D. Inman, and R. Dashwood, *J. Electrochem. Soc.*, **155**, E63 (2008).
125. X.-L. Zou, X.-G. Lu, W. Xiao, Z.-F. Zhou, Q.-D. Zhong, and W.-Z. Ding, *Journal of Shanghai Jiaotong University (Science)*, **18**, 111 (2013).
126. P. K. Tripathy and D. J. Fray, *Sustainable Industrial Processing Summit*, *Molten Salts and Ionic Liquids 2011*, Cancun, Mexico, **3**, 287 (2011), https://www.osti.gov/biblio/1042346.
127. S. Osaki, H. Sakai, and R. O. Suzuki, *J. Electrochem. Soc.*, **157**, E117 (2010).
128. V. E. Ri, Y.-J. Lee, B.-U. Yoo, H. Nersisyan, and J.-H. Lee, *ECS Meeting Abstracts*, Dallas, TX(IOP), **MA2019-01**, 2170 (2019).
129. M. Ramachandran and R. G. Reddy, *Journal for Manufacturing Science & Production*, **11**, 15 (2011).
130. M. Ramachandran and R. G. Reddy, *Annual Meeting Supplemental Proceedings*, *143rd Annual Meeting & Exhibition TMS 2014*, Warrendale, PA (Springer, Cham,) p. 57 (2014).
131. Q. Wang, J. Song, J. Wu, S. Jiao, J. Hou, and H. Zhu, *Phys. Chem. Chem. Phys.*, **16**, 8086 (2014).